

# FLIGHT DATA ANALYSIS OF POWER SUBSYSTEM DEGRADATION AT NEAR SYNCHRONOUS ALTITUDE

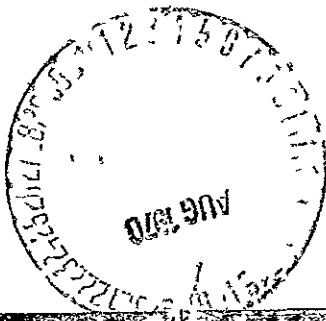
## THIRD QUARTERLY REPORT

CONTRACT NASW-1876

PREPARED FOR

NATIONAL AERONAUTICS AND SPACE ADMINISTRATION  
OFFICE OF ADVANCED RESEARCH AND TECHNOLOGY  
HEADQUARTERS, WASHINGTON, D C

**PHILCO** 



SPACE'S RE-ENTRY SYSTEMS DIVISION  
Philco-Ford Corporation  
Palo Alto, California 94303

FACILITY FORM 602

(ACCESSION NUMBER)

1130-35795

(THRU)

CR-169981  
(PAGES)  
(NASA CR OR TMX OR AD NUMBER)

(CODE)

03  
(CATEGORY)

Reproduced by  
**NATIONAL TECHNICAL  
INFORMATION SERVICE**  
Springfield Va. 22151

QQT-62451

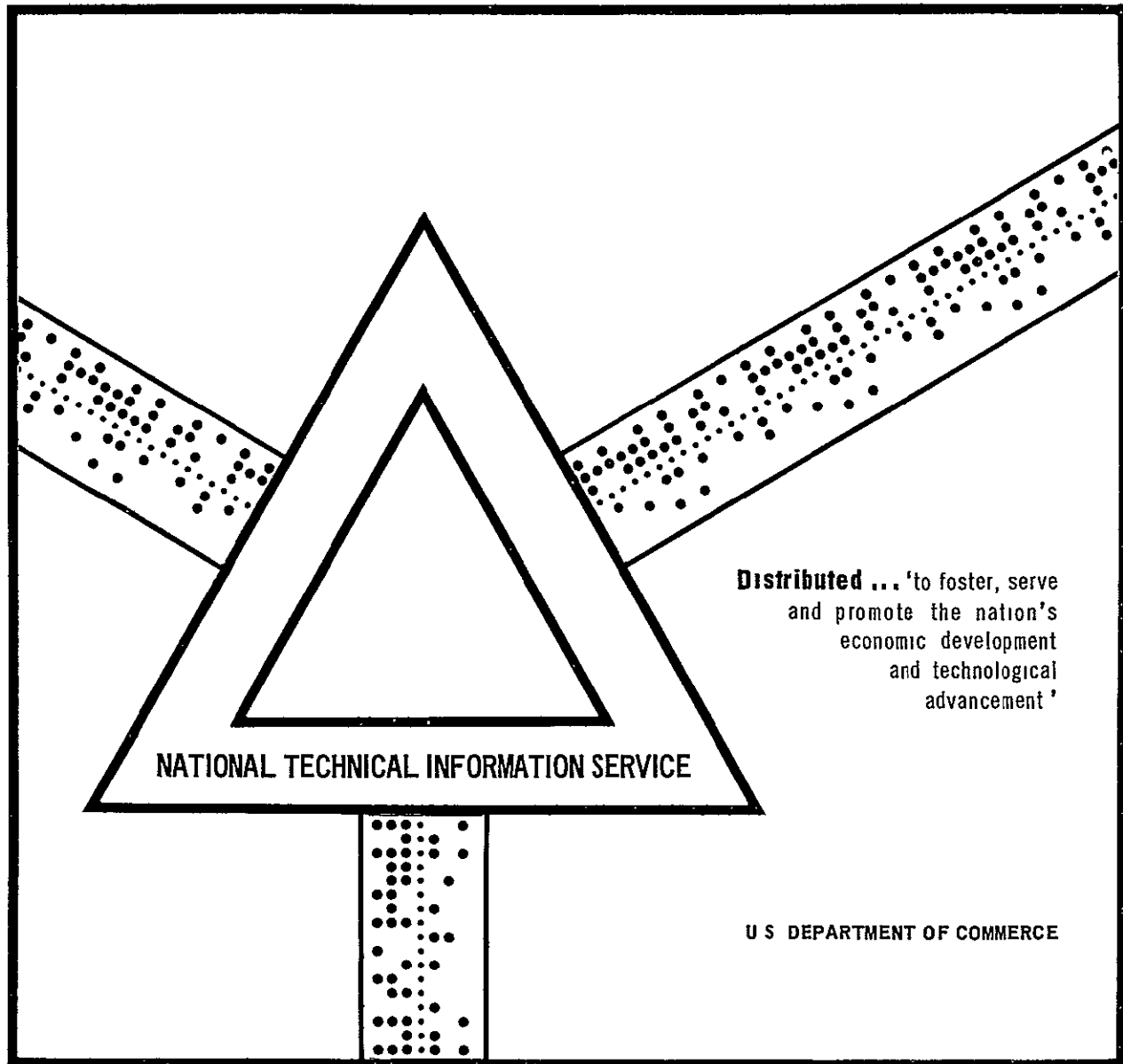
## ABSTRACT

A study of the solar arrays on 19 Air Force IDSCS satellites in near synchronous orbit is in progress. The best- and worst-case degradations projected to 5 years, due to all cell and non cell losses, are 10.6% and 15.6% for short circuit current and 1.7% and 5.7% for open circuit voltage. Calculated cell degradations, due to residual electrons and flare protons under the 20-mil coverslide shielding, indicate that maximum damage regions appear at electron energies near 0.7 meV and at proton energies near 3 meV. The updated ratio of electron to proton cell damage appears to be about 5.2. Best- and worst-case coverslide assembly losses, projected to 5 years, are estimated as 5% and 10%.

N70-35795

FLIGHT DATA ANALYSIS OF POWER SUBSYSTEM  
DEGRADATION AT NEAR SYNCHRONOUS ALTITUDE

Philco Ford  
Space & Re-Entry Systems Division  
Palo Alto, California



FLIGHT DATA ANALYSIS OF  
POWER SUBSYSTEM DEGRADATION  
AT NEAR SYNCHRONOUS ALTITUDE

THIRD QUARTERLY REPORT

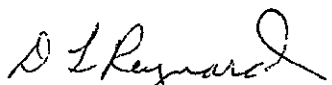
Contract NASW - 1876

Approved by

Prepared by

W. T. Picciano  
R. A. Reitman

  
R. J. Grant  
Program Manager

  
D. L. Reynard, Manager  
Power & Control Engineering Dept

Prepared For

National Aeronautics and Space Administration  
Office of Advanced Research and Technology  
Headquarters  
Washington, D C

## FOREWORD

This report concerns the electrical power subsystem performance of the Initial Defense Satellite Communication System.\* In particular, it details the on-orbit degradation of the satellite solar arrays. The work is sponsored by the National Aeronautics and Space Administration under contract NASW-1876.

The study is being conducted in the Power and Control Engineering Department of the Philco-Ford Space and Re-entry System Division at Palo Alto, California. This department is managed by Mr. D L Reynard. The program is under the overall technical direction of Mr. R. J Grant. Mr W T Picciano is responsible for the physical analysis and mathematical techniques employed in the study. Mr R A Reitman has implemented the computer programming and the automatic computer plotting of the program output.

This Third Quarterly Report generally updates and supplements the material presented in the previous two quarterly reports.\*\* The Final Report on the study, to be published July 15, 1970, will be inclusive.

\*Formerly Initial Defense Communication Satellite Program (IDCSP)

\*\*Flight Data Analysis of Power Subsystem Degradation at Near Synchronous Altitude, First Quarterly Report, Philco Ford Technical Report TR-DA2124, 3 October 1969 Second Quarterly Report, TR-DA2159, 5 January 1970

## TABLE OF CONTENTS

<u>Section</u>		<u>Page</u>
1.0	SUMMARY OF RESULTS	
1.1	Summary of Results	1-1
2.0	INTRODUCTION	
2.1	Background	2-1
2.2	Task Descriptions and Status	2-1
3.0	METHODS AND ANALYSIS	
3.1	Study of Anomalous Seasonal Variations and Scatter in Dot Plots	3-1
3.1.1	The Diode Intensity Factor	3-2
3.1.2	The Cosine Correction Factor	3-3
3.1.3	Zonal Imbalance	3-5
3.1.4	Data Scatter	3-7
3.2	Variation of the Cell Equation Parameters to Express Solar Cell Degradation	3-9
3.2.1	Other Solar Cell Equations	3-10
3.2.2	Parameterized Satellite Data	3-11
3.2.3	Verification of the Translation Assumption In Ground Data	3-11
3.2.4	Parameterization of Noncell Losses	3-23
4.0	DETAILED RESULTS	
4.1	Update of Observed Solar Flare Proton Spectrum	4-1
4.2	Calculated Radiation Degradation	4-3
4.3	Projected Observed Degradation to Five Years	4-8
4.4	Telemetry Error Analysis	4-12
4.4.1	Sources of Error	4-12
4.4.2	Worst-Case Approach	4-12
4.4.3	Influence of Worst-Case Instabilities on Degradation Data	4-13

## TABLE OF CONTENTS (Continued)

<u>Section</u>	<u>Page</u>
4.4.4 Observed Sensor Stabilities	4-13
4.4.5 Conclusions	4-14
4.5 Comparison of Other Flight Data	4-15

## LIST OF TABLES

<u>Table</u>	<u>Page</u>
4-1 Regression Parameters for Present Regression Curves	4-9
4-2 Satellite Past and Projected Degradation Ratios	4-10

## LIST OF ILLUSTRATIONS

<u>Figure</u>		<u>Page</u>
1-1	Observed and Projected Cell Short-Circuit Current Degradation	1-2
1-2	Observed, Projected and Calculated Cell Open-Circuit Voltage Degradation	1-3
1-3	Estimated Non-Cell Losses and Calculated Cell Short-Circuit Current Loss Projected to Five Years	1-4
2-1	Task Description Flow Diagram	2-3
3-1	Cosine Correction Factor vs Square Error	3-4
3-2	Zonal Imbalance Factor vs Square Error	3-6
3-3	IDSCS Parameter $I_L$	3-12
3-4	IDSCS Parameter A	3-13
3-5	IDSCS Parameter B	3-14
3-6	IDSCS Parameter R	3-15
3-7	IDSCS Parameter $I_0$	3-16
3-8	Ground-Irradiation Data Parameter $I_L$	3-17
3-9	Ground-Irradiation Data Parameter A	3-18
3-10	Ground-Irradiation Data Parameter B	3-19
3-11	Ground-Irradiation Data Parameter R	3-20
3-12	Relative Open-Circuit Voltage For Electron and Proton Irradiation	3-21
3-13	Relative Maximum Power for Electron and Proton Irradiations	3-22
3-14	Effect on Parameters A and B of Pure Non-Cell Loss	3-24
3-15	Effect on Parameter R of Pure Non-Cell Loss	3-25
4-1	Average Flare Proton Environment for 1967 and 1968	4-2
4-2	Residual Electron Differential Spectrum	4-4
4-3	Residual Proton Differential Spectrum	4-5
4-4	Product of Damage Constant and Differential Spectrum for Electrons	4-6
4-5	Product of Damage Constant and Differential Spectrum for Protons	4-7

## LIST OF ILLUSTRATIONS (Continued)

<u>Figure</u>		<u>Page</u>
4-6	Comparison of $I_{SC}$ Degradation	4-17
4-7	Comparison of $V_{oc}$ Degradation	4-18
4-8	Comparison of $P_{max}$ Degradation	4-19

SECTION 1 0

SUMMARY OF RESULTS

### 1.1 SUMMARY OF RESULTS

The primary objectives of this program are (1) to establish the quantitative degradation rates of the power subsystems of 19 IDSCS spacecraft in near synchronous orbit, (2) to investigate the degradation of the I-V characteristics of their solar arrays, (3) to investigate any anomalistic or unexpected behavior relating to environmental damage, and (4) to analyze all results such that the benefits of this flight experience can be applied to other current and future programs.

A significant aspect of our analytical results concerns the surprising variations observed in identical satellite solar arrays, both as to initial array outputs and to cell degradation rates on-orbit. Initial short-circuit currents and open-circuit voltages show a near Gaussian distribution and span 10.1% and 1.8%, respectively. This spread may be attributed to the random panel selection used in satellite construction and, in part, to telemetry sensor variations. When all initial parameters are normalized to unity, subsequent degradation levels over 5 years are again observed to span 5.0% for  $I_{sc}$ , and 4.0% for  $V_{oc}$ . Figure 1-1 presents best- and worst-case cell short-circuit current degradation curves, extrapolated to five years, for the first two IDSCS payloads (i.e., 15 satellites). All cell and noncell losses are included. The best- and worst-case endpoints are 0.894 and 0.844. Figure 1-2 presents similar open-circuit voltage curves, the best- and worst-case endpoints are 0.983 and 0.943. Figure 1-2 also includes a curve which corresponds to the theoretically calculated  $V_{oc}$  degradation, based on the updated radiation environment and best available damage coefficient data. This curve is observed to present an average path between the measured extremes.

Figure 1-3 presents the calculated  $I_{sc}$  degradation to cell alone due to radiation. Comparing this curve with the two extreme curves of Figure 1-1, we present the best- and worst-case estimations of noncell (i.e., coverslide assembly) losses projected to five years, the curves indicate endpoints of 0.954 and 0.900.

The products of the damage coefficients and residual spectra under the 20-mil coverslide indicate regions of maximum damage, for the on-orbit electrons this region is near 0.7 meV, and for the protons, near 3 meV. The ratio of electron-to-proton damage is about 5.2.

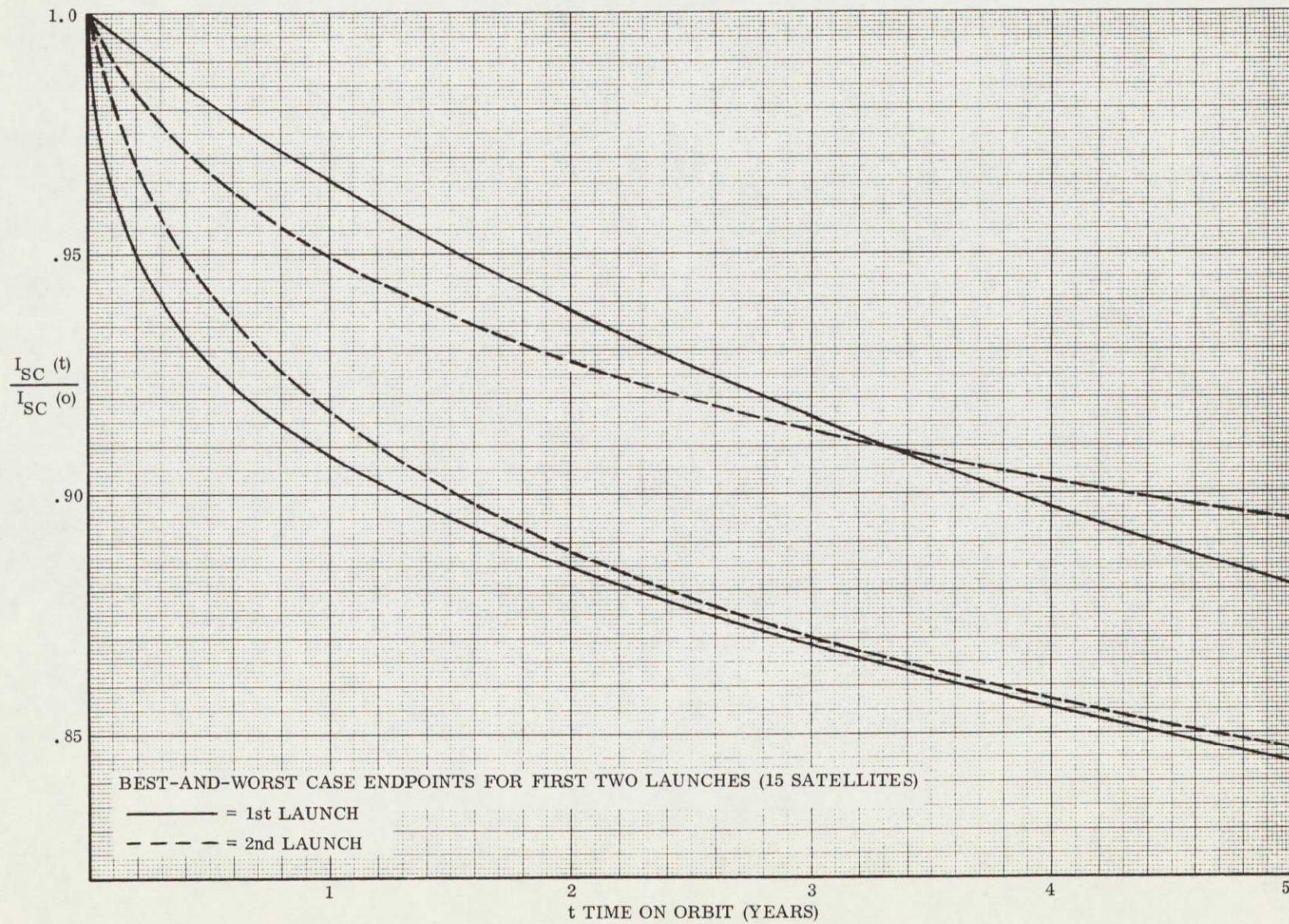


Figure 1-1 Observed and Projected Cell Short-Circuit Current Degradation

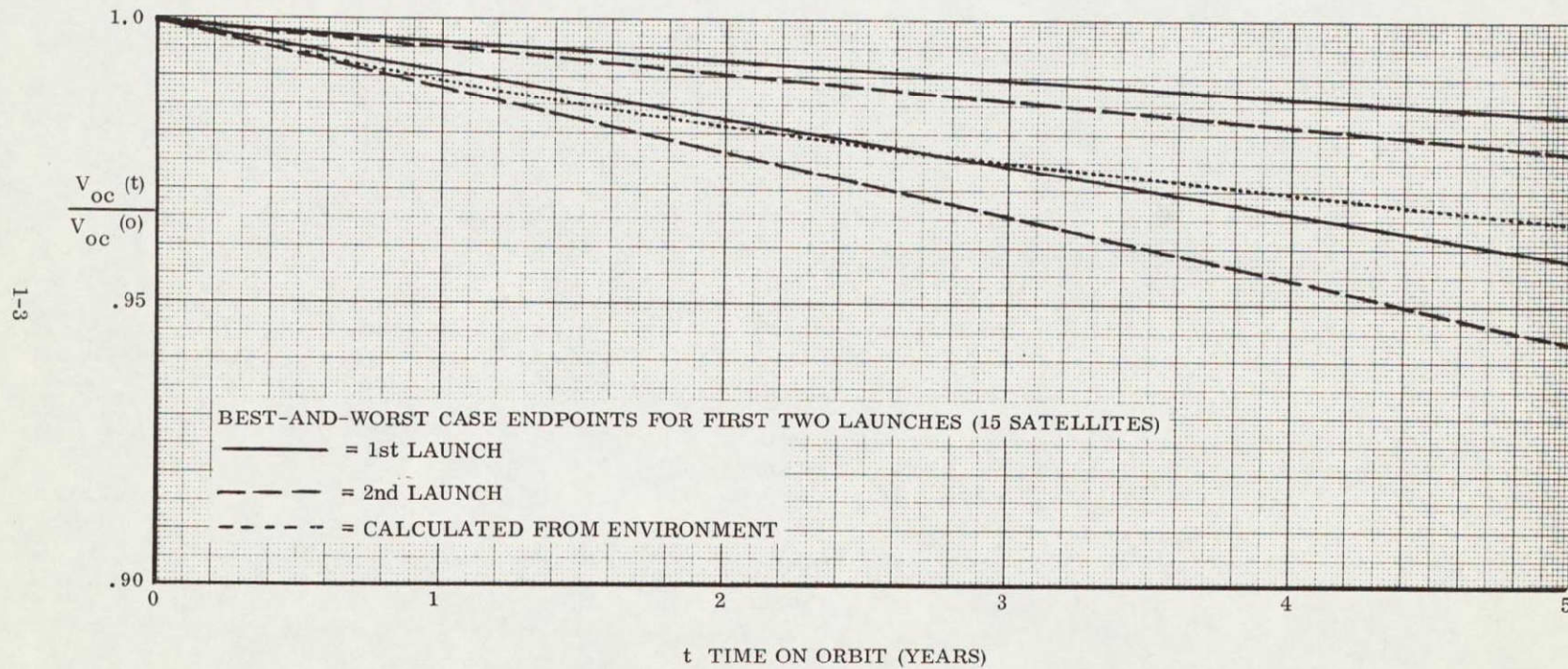


Figure 1-2 Observed, Projected and Calculated Cell Open-Circuit Voltage Degradation

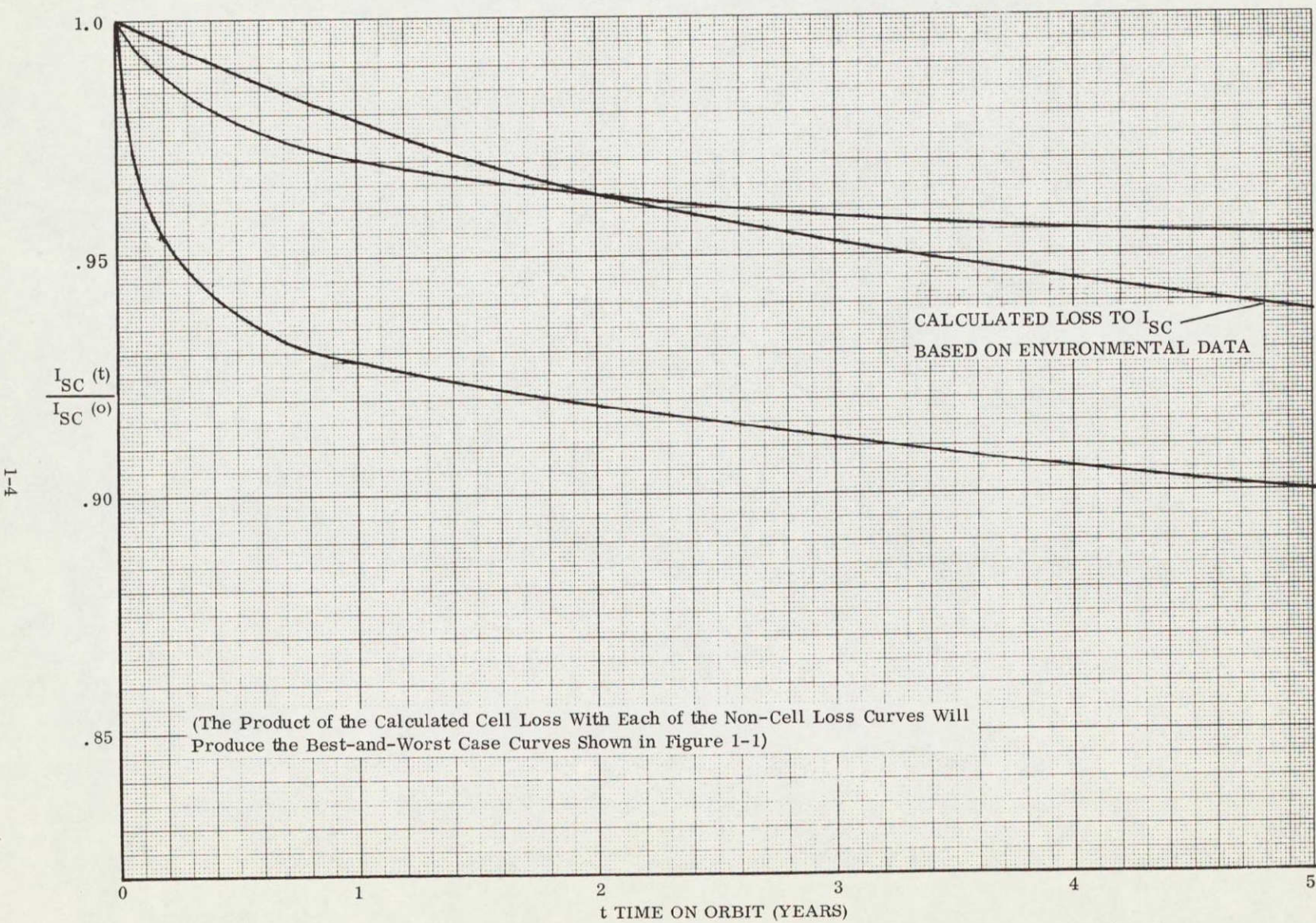


Figure 1-3 Estimated Non-Cell Losses and Calculated Cell Short-Circuit Current Loss Projected to Five Years

A study of the apparent periodic seasonal variation, superimposed on the output data in the dot plots, has examined three potential correction factors (1) an intensity dependence for the diode term in the solar cell equation, (2) a cosine modification term for incident light angles, and (3) a zonal imbalance factor in the average cell quality over the array. These factors, when implemented, were observed to reduce scatter (the sum of the squares of the deviations between the data points and the fitted function) by about 27%. No changes were observed in degradation rates or curve shapes.

A preliminary investigation of cell equation parameter variations in best- and worst-case satellites was initiated. The object is to present degradation data in a form which is particularly convenient for the array design engineer for generating complete I-V curves. The comparison of satellite parameter curves with ground irradiation and coverslide-loss parameter curves may provide, in addition, a new method to separate noncell from cell degradations and to assess the nature of the space radiation environment.

The final update of telemetry inputs and processed degradation data will appear in the next, and final, report. The Second Quarterly Report contains the most recent degradation dot plots published to date on this study.

SECTION 2 0

INTRODUCTION

## 2 1 BACKGROUND

On June 16, 1966, seven IDSCS satellites were successfully placed in near synchronous equatorial orbits. Subsequent to that launch, 11 additional IDSCS satellites and 1 Despun Antenna Test Satellite (DATS) were placed in similar orbits. A comprehensive picture of solar array and solar cell degradations at synchronous altitude is now being obtained. By virtue of the large number of identical satellites, it is possible to obtain a high statistical confidence in the results. Analysis will permit a study of solar flare damage during the period 1966 to 1969. Additional analyses will compare these flight results with ground irradiation data and other flight data in an attempt to explain any anomalistic behavior and allow more accurate sizing of future solar array designs.

Because of the importance of this orbit for both current and future missions, the high quality of the available telemetry data, and nature of the results which can be obtained from these data, it is felt that the conclusions of this study will be of considerable interest to both the array design engineer and the solid-state degradation theorist. The study covers three types of activity: Design Review and Data Reduction, Data Analysis, and Advanced Analysis. This study has been planned such that continuing periodic updates can be performed with a reasonably low level of effort.

The primary objectives of this program are (1) to establish the quantitative degradation rates of the power subsystems of 17 IDSCS spacecraft, (2) to investigate the degradation of the I-V characteristics of their solar arrays, (3) to investigate any anomalistic or unexpected behavior relating to environmental damage, and (4) to analyze all results such that the benefits of this flight experience can be applied to other current and future programs.

## 2 2 TASK DESCRIPTIONS AND STATUS

Figure 2-1 displays a block diagram/flow chart visual summary of the program. The unification of the individual tasks towards the overall program objectives is thus clarified. Each task block contains a status indication and a reference to the

location in this report of the detailed results applicable to that task. The notations FQR and SQR indicate First and Second Quarterly Reports. In general, all the completed task analyses will appear in Section 3, and all completed results in Section 4. The data span analyzed to date is 1200 days for the first launch satellites, 980 days for the second launch, and 815 days for the third. The data span of the final report will be approximately 1460, 1240, and 1075 days, for the respective launches.

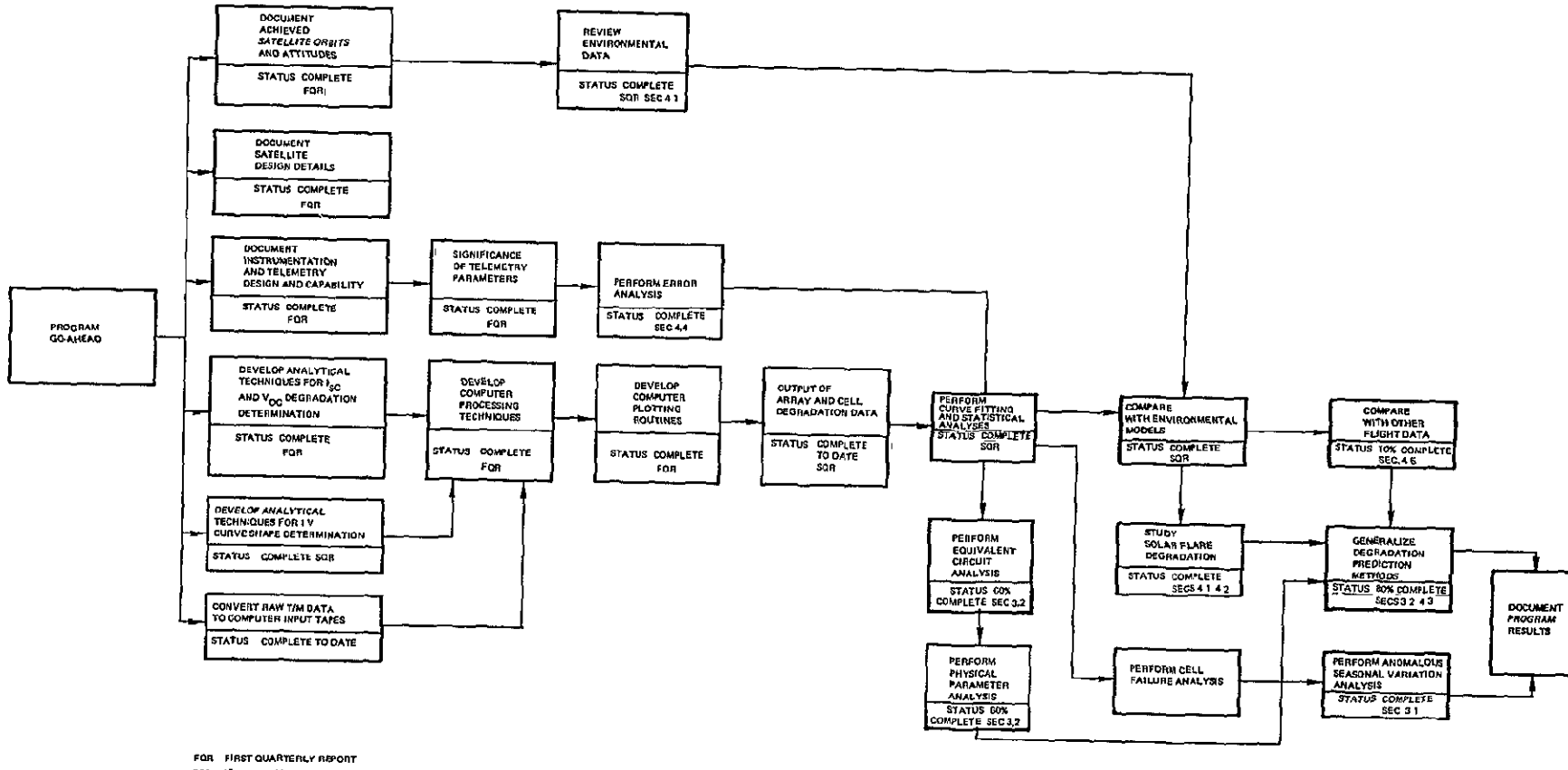


Figure 2-1 Task Description Flow Diagram  
(Includes Status and Reference Indications)

SECTION 3 0

METHODS AND ANALYSIS

### 3.1 STUDY OF ANOMALOUS SEASONAL VARIATIONS AND SCATTER IN DOT PLOTS

A visual examination of the computer dot plots of the degradation ratios versus time has suggested that a superimposed sinusoidal variation rides on the overall trend. Three potential sources of systematic periodic error have been investigated.

- a The Diode Intensity Factor. The solar cell equation is based on a mathematical model which, in its simplest form, is a current generator in parallel with a diode. Variation of incident light energy has been assumed to affect the  $I_L$  term only, whereas the remaining collection of terms (the diode) also varies slightly with intensity.
- b The Cosine-Correction Factor. Lambert's Law indicates a direct equivalence between the illumination of a plane surface and the cosine of the angle between the incident light and the surface normal. In a solar cell, however, the light-generated current varies somewhat depending on where in the cell minority carriers are produced by absorbed light. The larger the incidence angle, the closer to the junction the carriers will be produced, but the higher the probability of absorption in the heavily doped surface region. The former aspect is an enhanced contribution to current and the latter, a loss. Thus, a plot of  $I_L$  versus the cosine of the angle of the incident light deviates slightly from the linear Lambert Law.
- c Zonal Imbalance. Satellite geometry produces three distinct zones on each vehicle. During one-half of the year, the upper zone has a more favorable sun angle for producing power than the lower zone, and vice versa for the other half of the year. If, by chance, the average solar cell used in assembling the panels in one zone were slightly better, relative to the average cells used in the other zone, a periodic power output variation would result.

### 3.1 1 The Diode Intensity Factor

Two diode intensity corrections were derived from measurements made in the Philco-Ford Space Power Laboratory. The data were in the form of complete I-V curves at incident light angles varying between 0° and 80°. To avoid cosine correction effects, short-circuit current ratios were read from the curves and used as intensity ratios with no reference to the corresponding light angles. The major deviation between current as calculated from the applied solar cell equation and the data appeared between  $V_{oc}$  and 0.8  $V_{oc}$  at lower intensities. This deviation suggested a correction to the cell parameter, A. A appeared to vary with the logarithm of the intensity ratio,  $\phi$ . Plotting A versus  $\phi$  on semi-log paper produced the relation.

$$A = A_0 - 0.1557 \ln \phi.$$

Other experimenters have reported a diode term dependence varying with  $\ln \phi$ , but the above relation does not produce this. In the standard solar cell equation, the quantity  $I_o$  essentially multiplies the diode term, since  $I_o \equiv \exp(-A/B)$ , the diode term would effectively be multiplied by a correction factor of  $\phi$  raised to a fixed power

$$\phi^{0.1557/B} \simeq \phi^{0.4}$$

A second correction factor, based on the same data, was derived in terms of  $A/A_0$ ,

$$A/A_0 = 1.0433 - 0.04365 \phi + 0.032 \exp(-4.513 \phi)$$

This factor produced excellent agreement with the lab data and was subsequently computerized into the analysis program. Test cases were run on first launch satellites and the resultant square error compared with earlier runs. No improvement was observed and the correction was judged insignificant.

### 3.1.2 The Cosine Correction Factor

A number of sources were reviewed to obtain information on cosine modification functions. Data taken at Philco-Ford, at Heliotek, and at Johns Hopkins University<sup>(1)</sup> generally indicated a negative correction to the cosine for large angles and a positive correction for near normal angles, TRW data<sup>(2)</sup> indicated a universal negative correction which was greatest near 70°. A reasonable general form for the Philco-Ford and Johns Hopkins data was a simple sine function modified by an additive linear function which could pivot about the 0° point. More accurate correction functions could be derived to fit any one set of data, but the variations and inconsistencies among the different sources indicated that knowledge of this function was too uncertain to warrant much added sophistication. Our function was introduced into the analysis program (modifying all individual solar cells), the program run with satellite data, and the resultant scatter measured. The parameters of the function could be varied until the sum of the square errors of the degradation ratio points about their fitted mean was minimized. Figure 3-1 shows the first result of this type of calculation with satellite No. 9312. Defining  $u$  as  $\cos \theta$ , the corrected  $u$  was of the following form

$$u' = u - A \sin 2\pi u + b(1 - u)$$

The variation of  $A$  produced minimum scatter at about  $A = 0.035$ , with  $b = 0$ . Comparing the magnitude of this maximum correction to the other available data (taken on single cells in ground laboratories), we obtain the following

(1) Solar cell output as a function of Angle of Incidence, data taken by John Hopkins Applied Research Laboratories and quoted in a Heliotek information release, no date (circa 1965)

(2) TRW, Solar Array, Minimum Output Characteristic Computer Program, Appendix A, IOC 9361 4-237, 29 December 1964

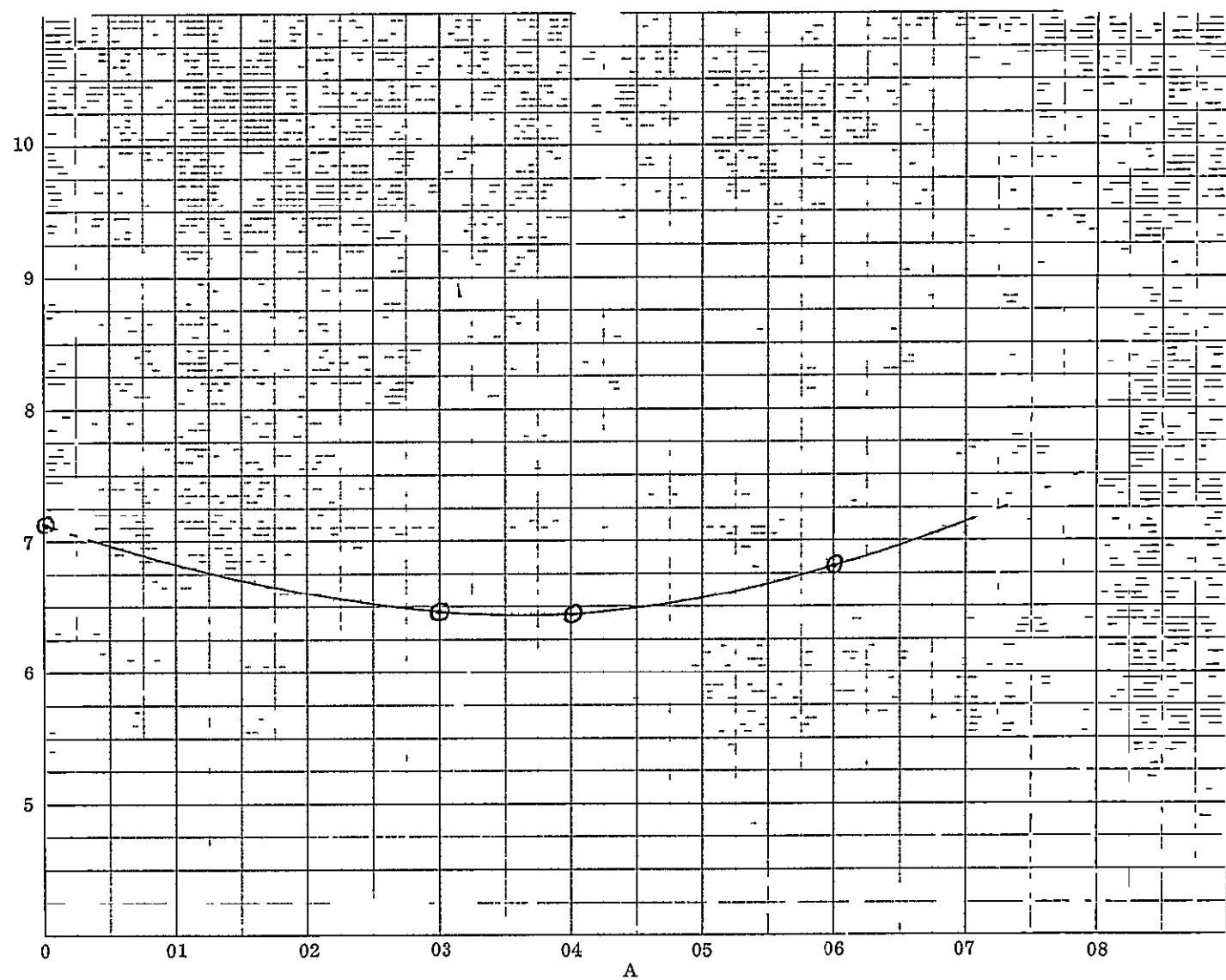


Figure 3-1 Cosine Correction Factor vs Square Error

<u>Source</u>	<u>Max Correction to u</u>	<u>At u =</u>
This Study	-0 035	0 25
	+0 035	0 75
Philco Lab Data	-0 034	0 23
	+0 017	0 87
Johns Hopkins/Heliotek	-0 054	0 26
	+0 030	0 77
TRW	-0 050	0 27

There appears to be some consistencies despite the variations. Time has not permitted an iteration on b or other detailed studies in this area. The 10% reduction in scatter observed in Figure 3-1 is significant, and indicates the potential of an analysis program such as this to extract subtle behavior factors from masses of crude telemetry data. However, no major changes in degradation rates, curve shapes, nor end-of-life to start-of-life ratios were effected in the overall data. The correction factor did have the effect of translating the curves slightly, in comparison to the previously published curves, and a decision is still pending whether the factor should be retained or removed from the program. If the factor is retained, our final update would necessitate a rerun of all the previous data in addition

### 3.1 3 Zonal Imbalance

The average  $I_L$  output of Zone I solar cells was adjusted mathematically to test two hypotheses: the average quality of cells might differ by a few percent between Zones I and III, and/or a cell failure or a single anomalously darkened coverslide might upset average zonal balance. The surprising 10% spread in initial array short-circuit current values (in the identically constructed 19 satellites) would indeed seem to open the possibility of an extremely probable zonal imbalance. Figure 3-2 presents the resultant square error versus an imbalance factor run on satellite No. 9312, a 3.5% imbalance is observed to reduce data scatter by 17%. Once again, the overall degradation ratio is changed

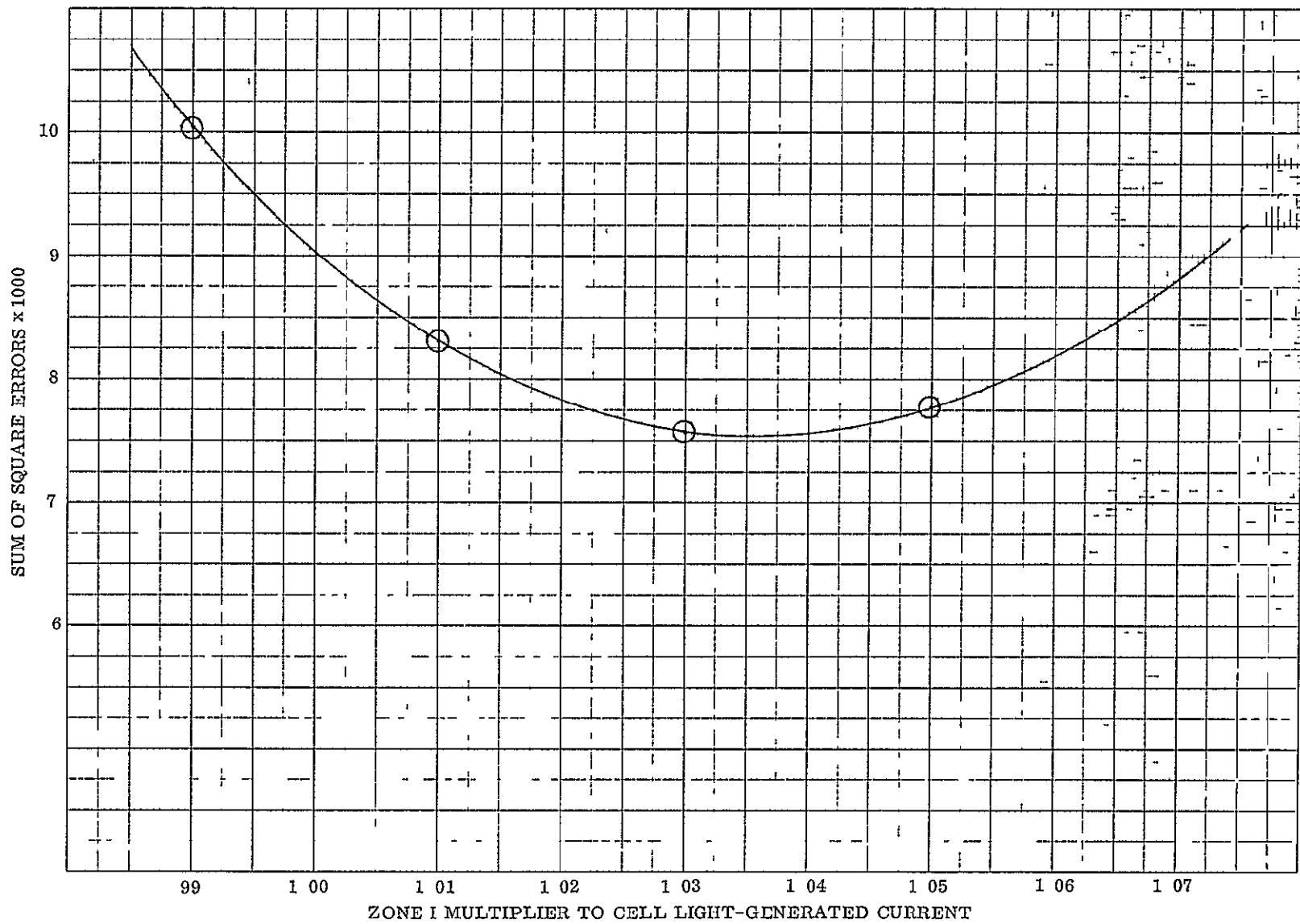


Figure 3-2 Zonal Imbalance Factor vs Square Error

insignificantly ( $I_{sc}/I_{sc}^0$ ) reads 0.4% higher at 5 years with the 3.5% imbalance.) The utility of deriving this zone factor for each satellite is thus questionable.

### 3 1 4 Data Scatter

It is interesting to note that a single cell failure or anomalously darkened coverslide<sup>(3)</sup> in Zones I or III would effect an approximate imbalance in average output of about

$$100 \left(1 - \frac{31}{32}\right) \% = 3.1\%$$

This estimation is very close to the zonal imbalance factor derived above. The same cell failure situation could also cause an instantaneous maximum fluctuation of approximately

$$100 \left[1 - \frac{32(1 + \cos 23^\circ + \cos 68^\circ)}{32(1 + \cos 23^\circ + \cos 68^\circ)/\pi}\right] \% = 4.3\%$$

The cosines above represent approximate zonal light incidence angles at equinox, and the fraction denominator is roughly the number of projected strings contributing current on the sunlit side. Comparing this maximum fluctuation to the scatter histograms which have been run on all the satellites as part of the regression analysis, we observe that 98% of the scatter lies within 4.3%. Moreover, the 2% collection of deviant points usually occur at eclipse period times when temperature excursion data are probable in our inputs.

These observations are mentioned to show that the consequence of a single cell or coverslide failure could explain both the sinusoidal seasonal variation and the magnitude of the data scatter. When telemetry data was inputted into the program, however, efforts were taken to use peak values only when these were clearly evident.

---

(3) See footnote No. 4 on page 4-61 of the Second Quarterly Report on this study regarding anomalous darkening

This procedure was followed to eliminate, as best as possible, the fluctuations and general effects of an array cell failure. It appears far more probable at this writing, that the actual explanation is primarily zonal imbalance with a number of contributing secondary factors that a further in-depth study could uncover. Since overall degradation results are not altered by the reduction of the scatter, there appears to be little justification for the pursuit of such a study at this time.

### 3 2 VARIATION OF THE CELL EQUATION PARAMETERS TO EXPRESS SOLAR CELL DEGRADATION

This section presents preliminary results of the work currently in progress regarding the expression of degradation data in parametric form. The parameters referred to are the fixed constants which appear in the solar cell equation and which, as a group, establish a unique shape for a cell I-V curve. The term solar cell equation means any of the forms, inversions, or approximations of the mathematical model which adequately expresses the current versus voltage behavior of a particular solar cell to the required degree of accuracy. The intent of this effort is the development of an alternative method for the presentation of solar cell degradation information, a method which particularly simplifies the task of the array design engineer.

The standard lumped-parameters equation for silicon solar cells is usually written,

$$I = I_L - I_o \left\{ \exp \left[ \frac{q(V + IR)}{nKT} \right] - 1 \right\} - \frac{V}{p},$$

where the notation has been defined previously<sup>(1)</sup>. The section continues with a brief discussion of two other useful solar cell equations to which parameterized degradation data might ultimately be applied. The IDSCS behavior, as observed in this study, is then presented in terms of parameters which vary with time on-orbit. Because certain portions of IDSCS telemetry data are not yet available, a tentative simplifying assumption is introduced to enable preliminary calculation of the satellite parameters. When this assumption is checked against known ground irradiation data, it proves to be quite accurate, especially for the low fluences of interest to this program. One of the consequences of applying this assumption to satellite data, however, is that noncell losses (i.e., coverslide assembly darkening) will unavoidably be included in the same process. This aspect is briefly addressed and the section concludes with a somewhat unexpected realization that the parametric approach may be a new tool in the task of separating cell and noncell degradations.

(1) W T Picciano, Appendix A, First Quarterly Report, 3 October 1969

### 3.2 1 Other Solar Cell Equations

When recent vintage 2 x 2 cm silicon N/P cells are under consideration, the very simple inverted equation,

$$V = A + B \ln (I_L - I) - IR,$$

may suffice for preliminary design studies. The parameters, A and B, represent collections of the above standard parameters and have been defined earlier<sup>(1)</sup>. Given A, B,  $I_L$ , and R as a function of time, a complete cell I-V curve and a complete array I-V curve may quickly be generated. Radiation degradations (both cell and noncell), temperature effects, and light variations may all be accommodated in these parameters. In the case of the inverted equation above, it can be shown that knowledge of  $I_{SC}$ ,  $V_{OC}$ , and the values of the current and voltage at the maximum power point,  $I_m$  and  $V_m$ , is sufficient to compute all the equation parameters<sup>(2)</sup>.

IDSCS cells are 1 x 2 cm N/P boron-doped, phosphorous pentoxide-diffused silicon cells of 1964 vintage and, unfortunately, possess a shunt resistance of 350 to 500 ohms which cannot be neglected. A more general form of the cell equation,

$$I' = I_L - \exp \left[ \frac{V(1 - R/P) - A + I'R}{B} \right],$$

which has been discussed previously, will be assumed to apply. The above equation, with  $I' = I + V/P$ , can be written explicitly by a semi-iterative approximation to produce values of  $I = I(V)$  which agree with the standard lumped-parameters equation to within  $\pm 0.04$  milliamps<sup>(1)</sup>. Methods of calculating the

---

(2) W T Picciano, Determination of the Solar Cell Equation Parameter From Empirical Data  
Energy Conversion, Vol 9, pp 106, March 1969

equation parameters from I-V data have been presented in this study and elsewhere<sup>(3, 4, 5)</sup>

### 3.2.2 Parameterized Satellite Data

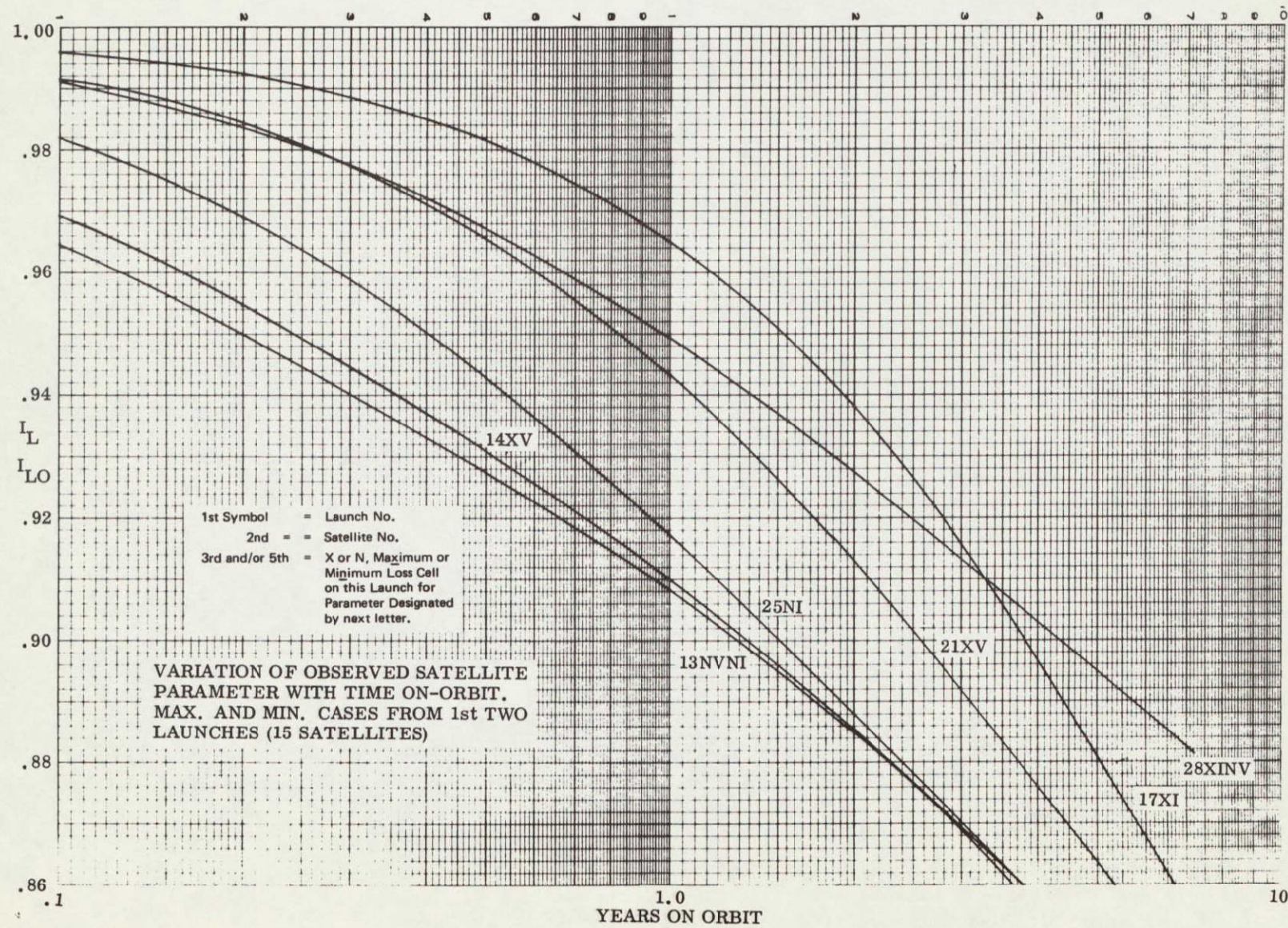
Figures 3-3 through 3-7 present a preliminary compilation of IDSCS parameters applicable to the best- and worst-case  $V_{oc}$  and  $I_{sc}$  curves from the first two launches (15 satellites). These results are preliminary because recent eclipse entrance data, which provide array "knee" region information, have not yet been forwarded to us by the Air Force. In lieu of these data, we have tentatively assumed that no knee rounding occurs, i.e., that degradation on-orbit produces simple translations of the cell I-V curve along current and voltage axes. Evidence indicates that this approximation may actually be quite good, peak radiation damage regions appear to occur between residual electron energies of 0.5 and 1.0 meV, and between residual proton energies of 2 and 4 meV. (See Section 4.2.) Published ground irradiation data indicate that cell degradations at these energies can be very adequately represented by simple curve translations.

### 3.2.3 Verification of the Translation Assumption In Ground Data

Figures 3-8 through 3-11 present the current status of a parametric representation of the Reynard<sup>(6)</sup> data on 0.6, 0.8, and 1.0 meV electron irradiations, and on 2.7 meV proton irradiation. These curves have been derived from  $I_{sc}$  and  $V_{oc}$  data only, assuming the translation approximation. Figures 3-12 and 3-13 show the resultant  $V_{oc}$  and  $P_{max}$  behavior recalculated from the parameters

---

- (3) W T Picciano, Appendix B, First Quarterly Report, 3 October 1969
- (4) K L Kennerud, A technique for Identifying the Cause of Performance Degradation in Cadmium Sulfide Solar Cells, Proc 4th IECEC, September 22-26, 1969, p 561
- (5) M J Barrett, Synthesis of Solar Cell Parameters (Sec III), an Analytical Review of the ATS-1 Solar Cell Experiment, Second Periodic Progress Report, Contract NAS 5-11663, Exotech Corp., June 15 1969
- (6) D L Reynard, Proton and Electron Irradiation of N/P Silicon Solar Cells, Contract AF 04(647) 787, Lockheed Rpt LMSC 3 56-65-4, 12 April 1965

Figure 3-3 IDSCS Parameter  $I_L$

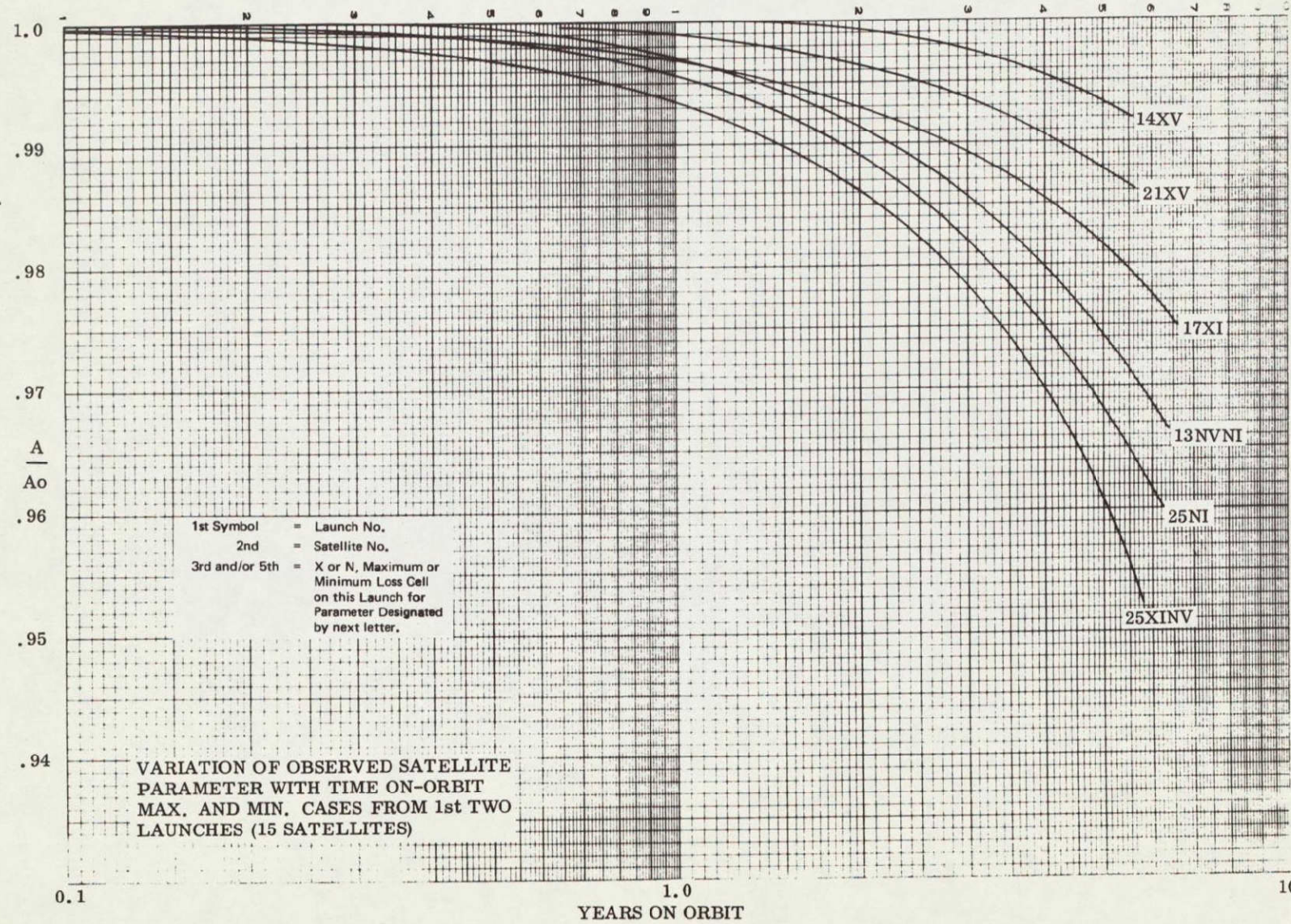
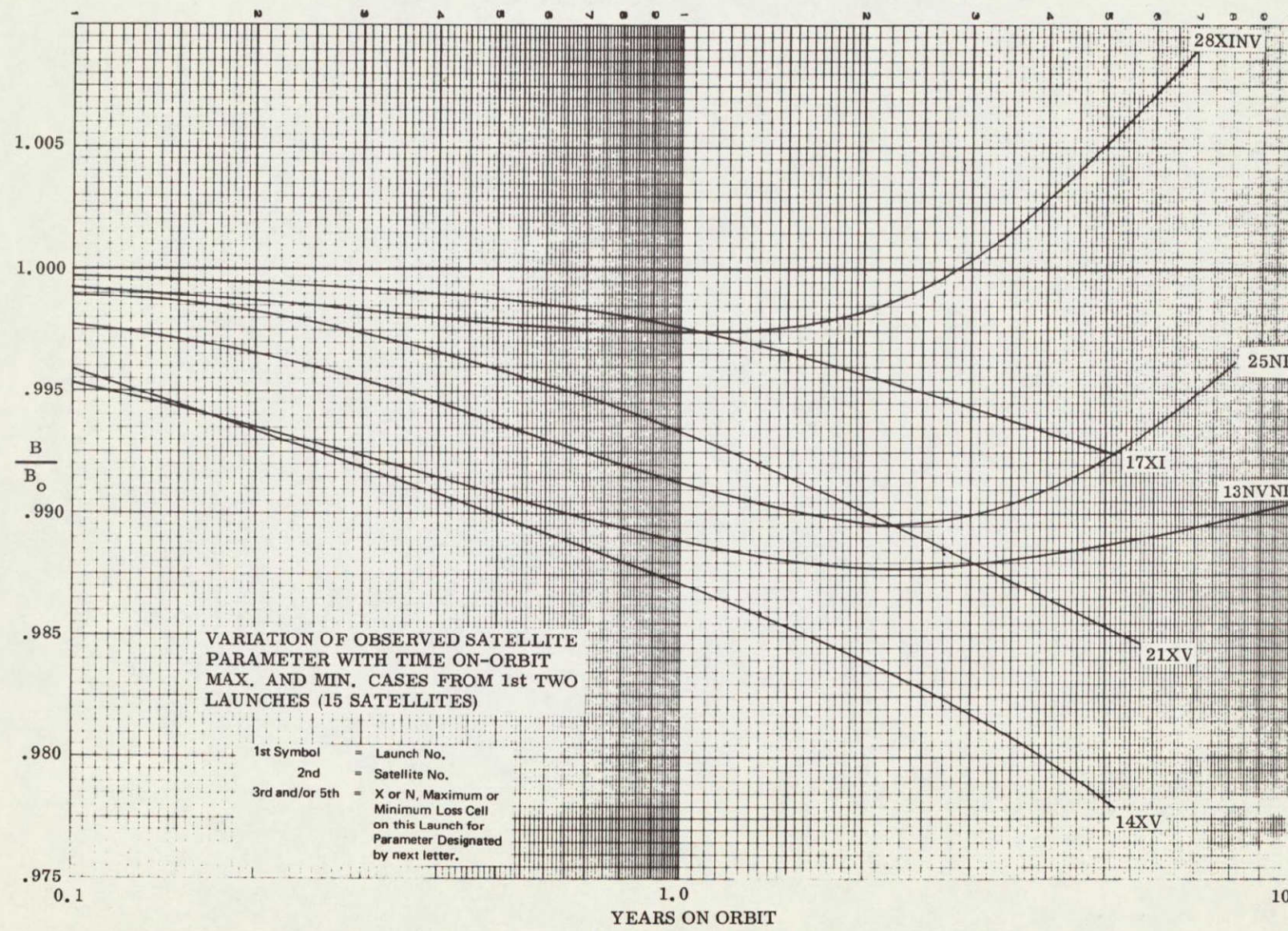


Figure 3-4 IDSCS Parameter A



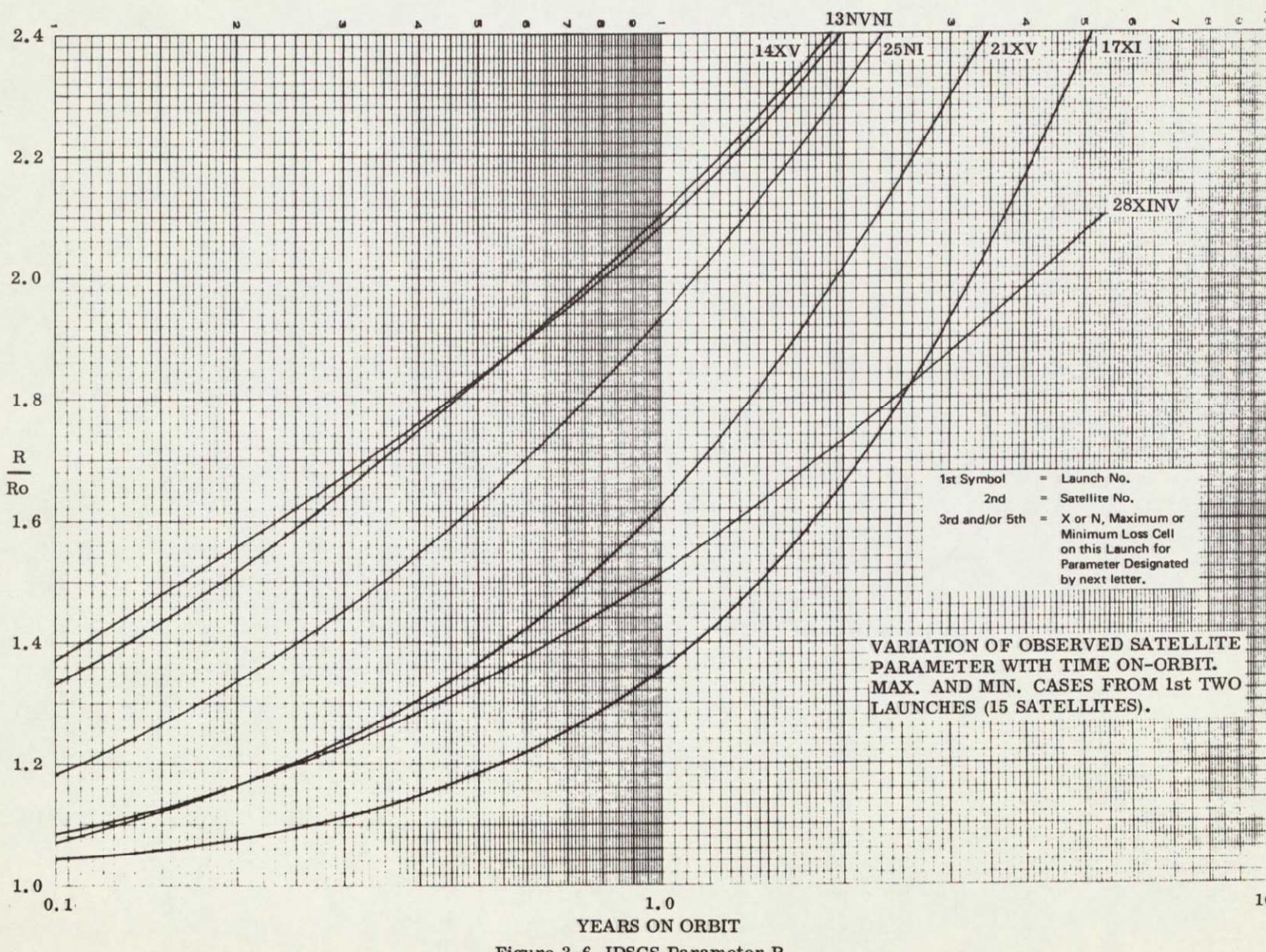
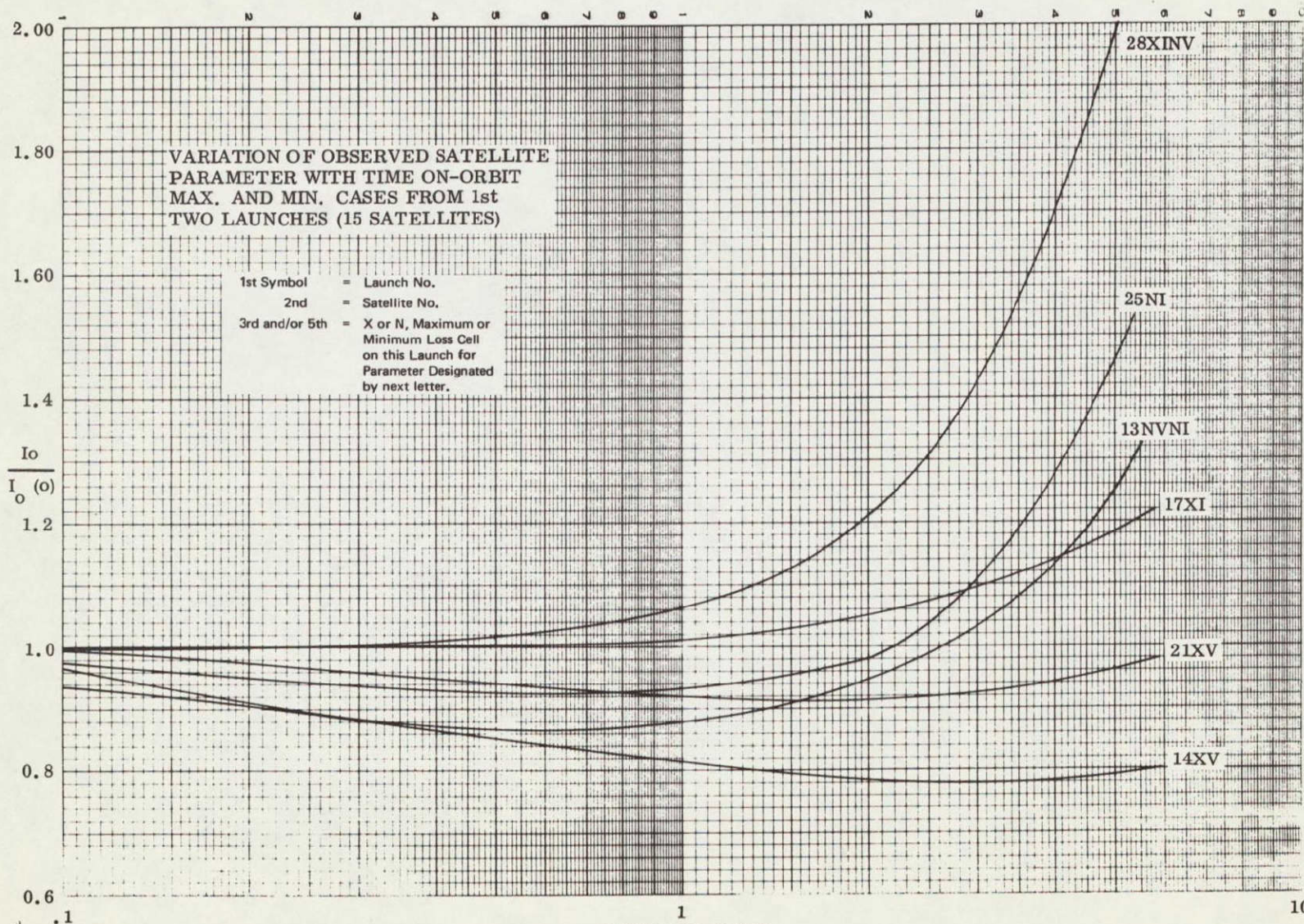
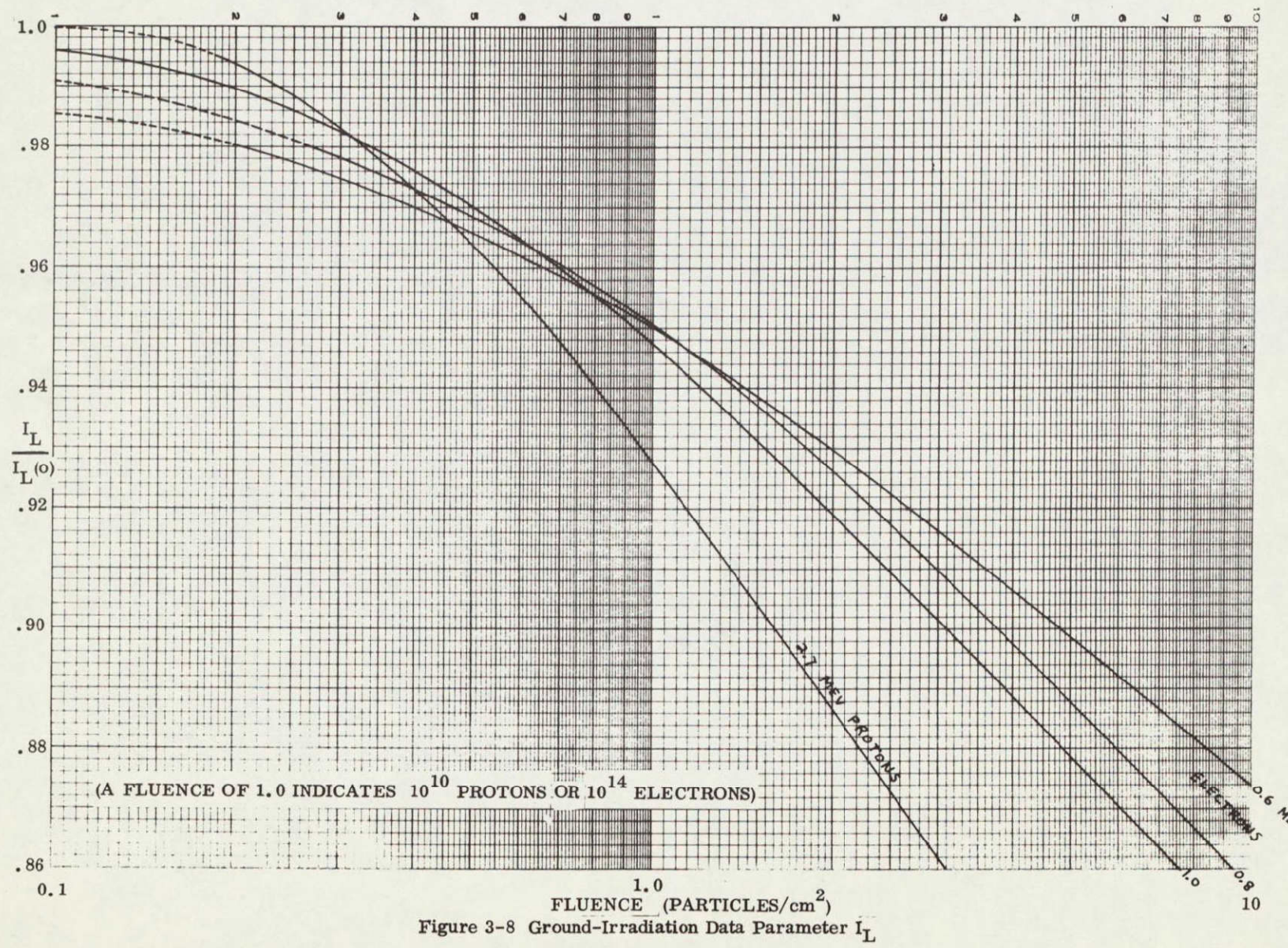


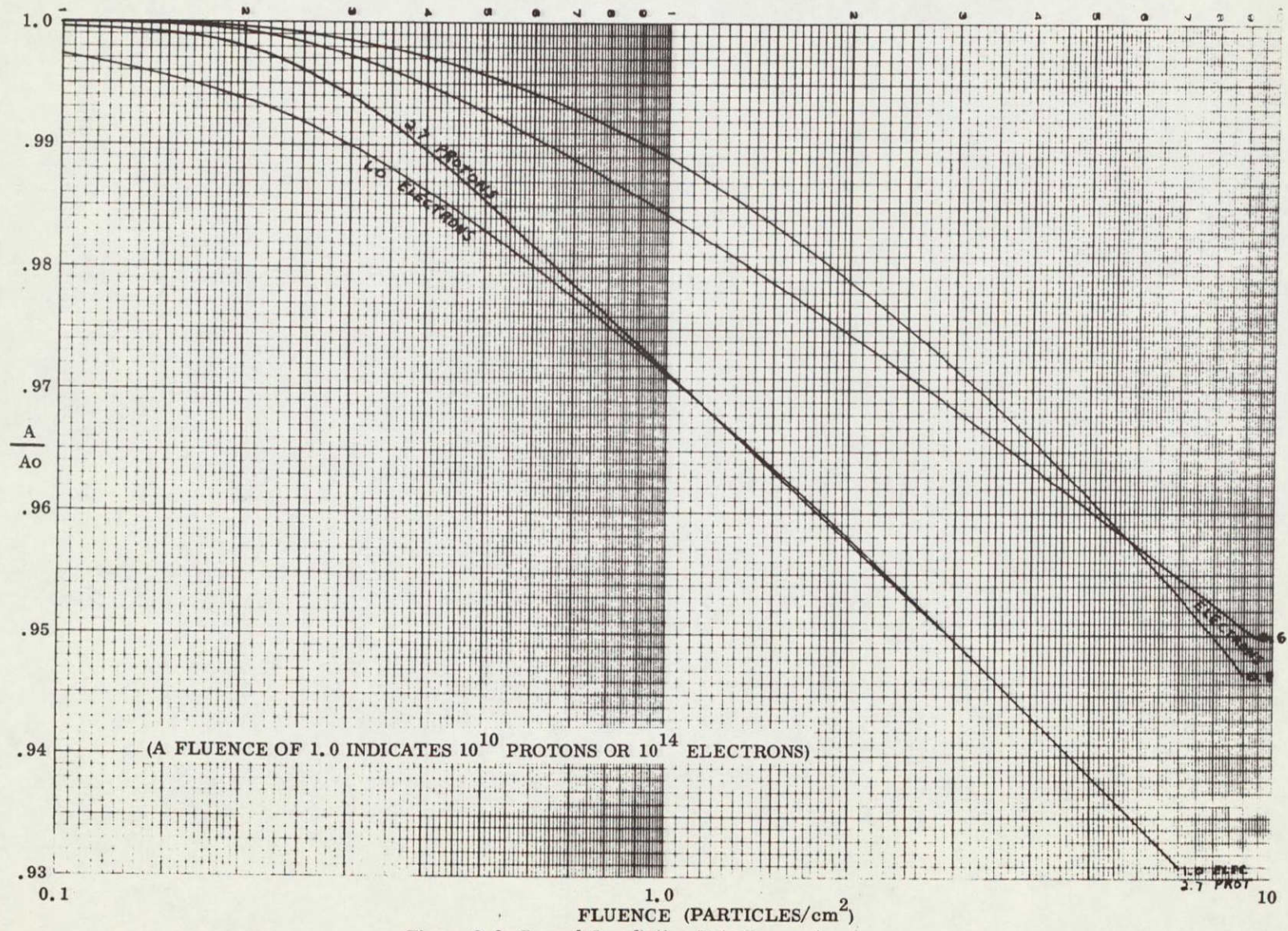
Figure 3-6 IDSCS Parameter R

Figure 3-7 IDSCS Parameter  $I_0$

3-17

Figure 3-8 Ground-Irradiation Data Parameter  $I_L$ 

TR-DA2179



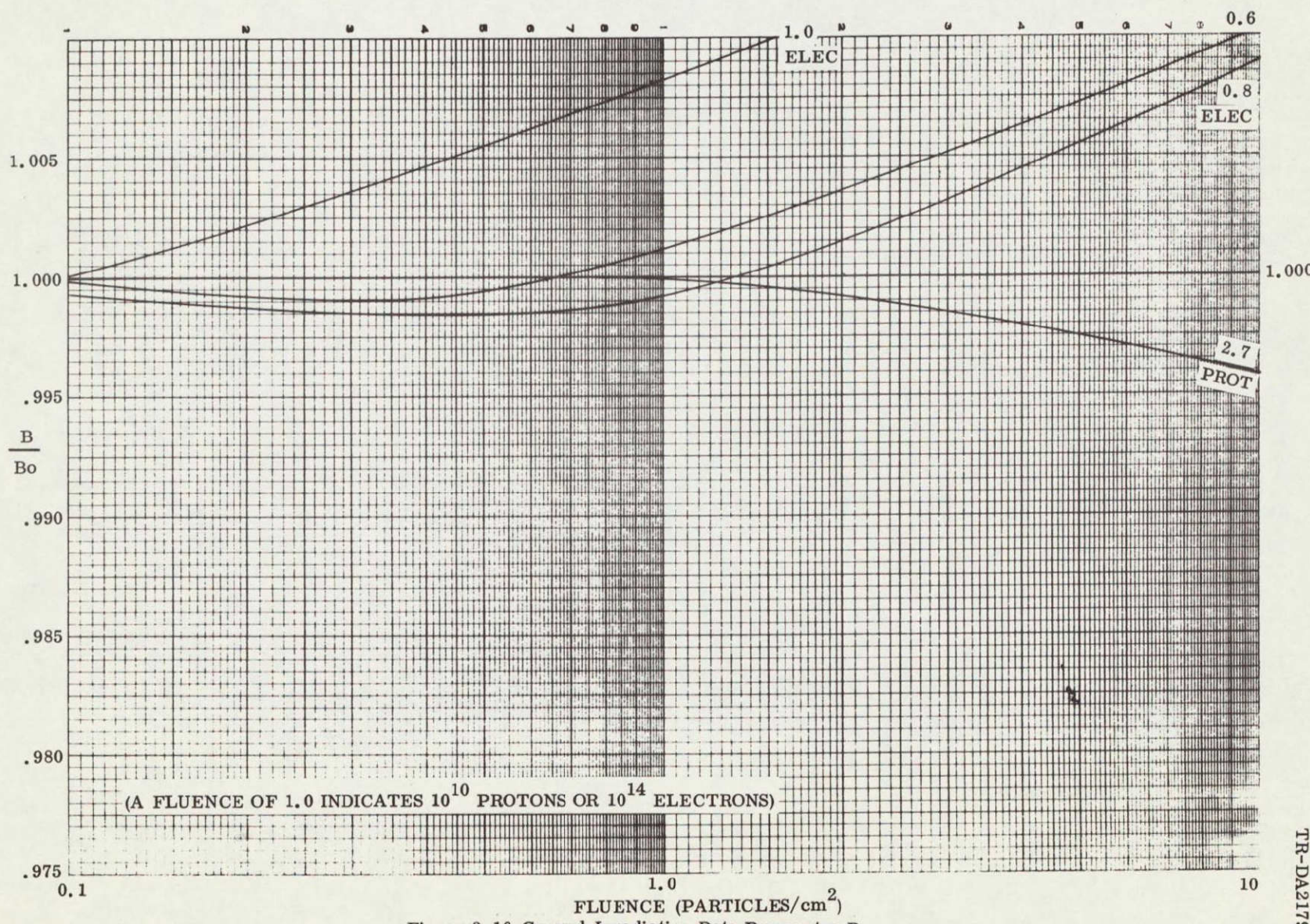


Figure 3-10 Ground-Irradiation Data Parameter B

TR-DA2179

3-20

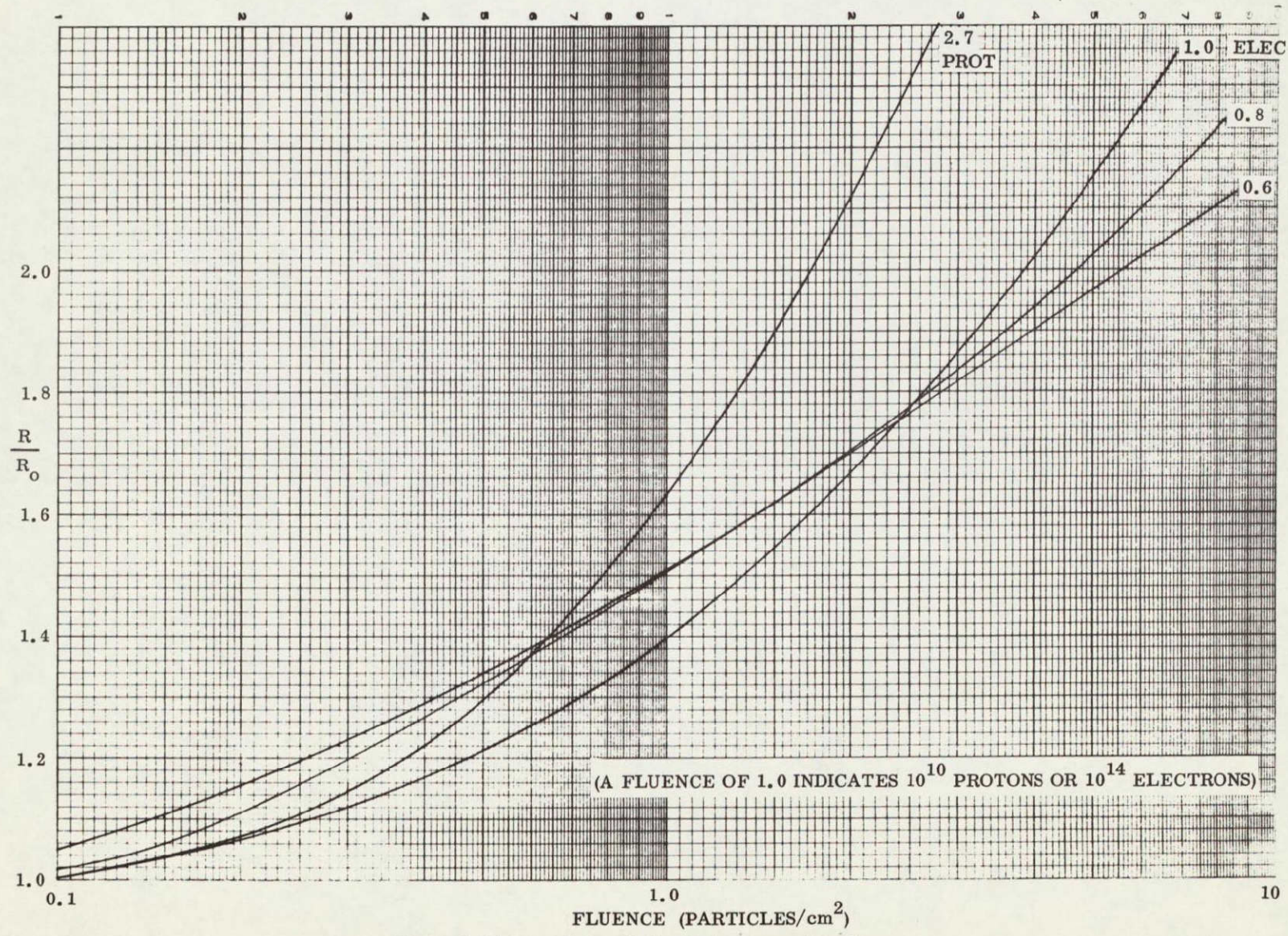


Figure 3-11 Ground-Irradiation Data Parameter R

TR-DA2179

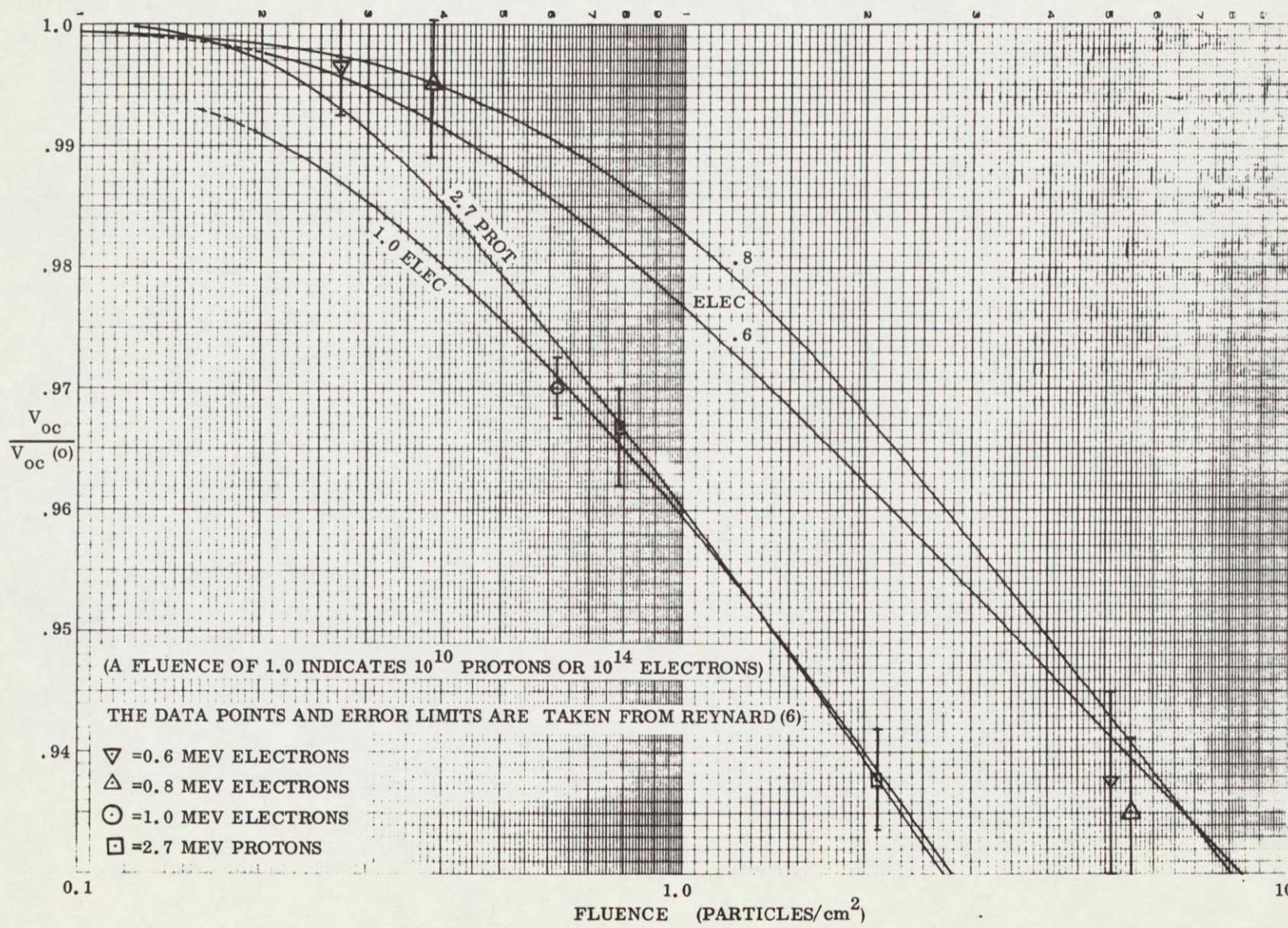


Figure 3-12 Relative Open-Circuit Voltage For Electron and Proton Irradiation

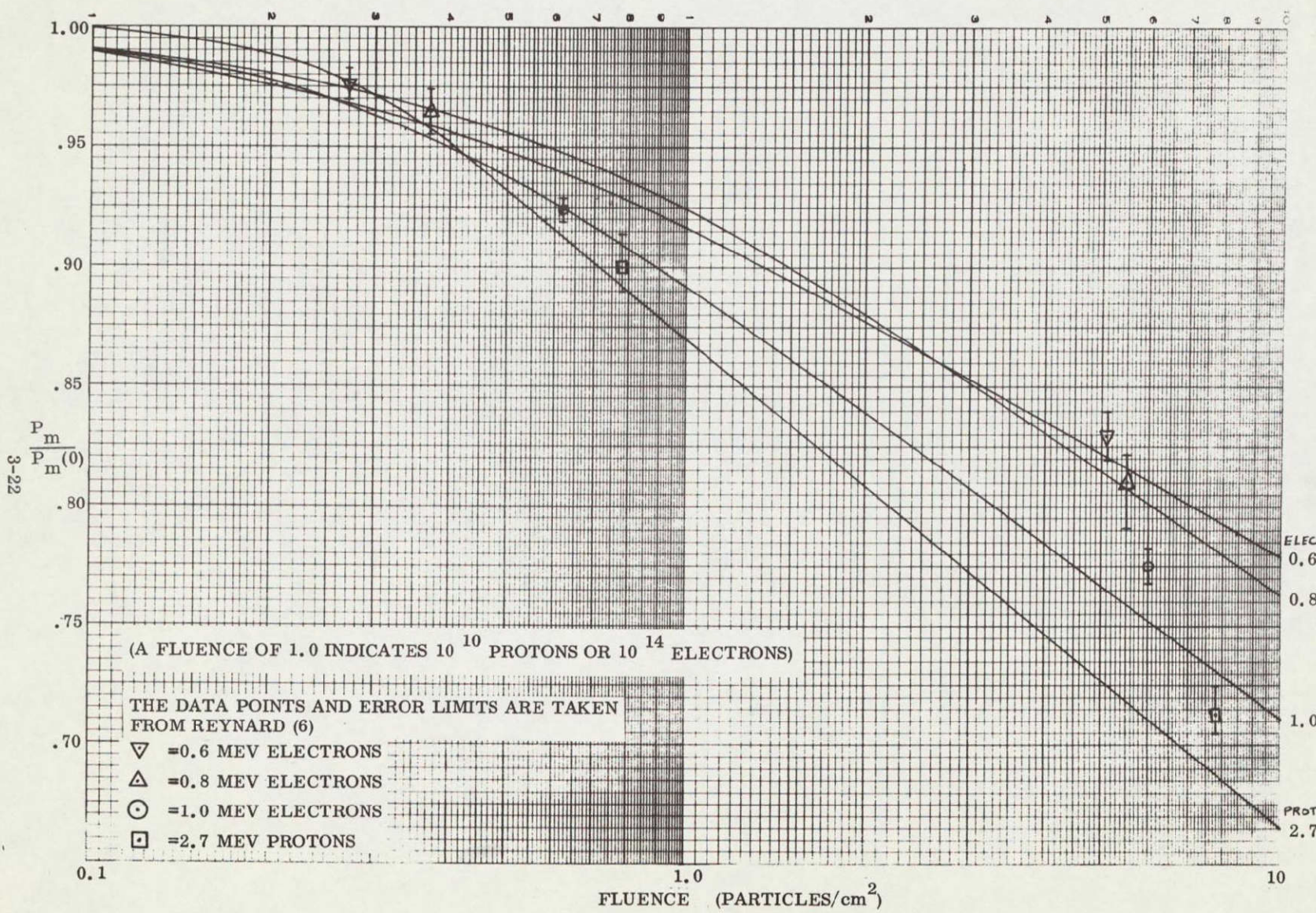


Figure 3-13 Relative Maximum Power for Electrons and Proton Irradiations

TR-DA2179

The agreement is excellent, especially at the low fluences of interest to this program (Discrepancies of 0.5 to 2.0% are currently observed at the higher fluences because time has not permitted iterations within the error limits of the Reynard data) The variations of the parameter B (Figure 3-10) are presented exactly as derived, but the presence of the very small negative dip in the electron curves might prove fallacious

### 3.2.4 Parameterization of Noncell Losses

The parametric plots of the satellite data result directly from the regression functions derived in the Second Quarterly Report. Shunt resistance,  $P$ , has been held constant at 370 ohms. No separation of cell and noncell damage has yet been attempted in the parameterization. It is of interest, however, to examine the effects on  $A$ ,  $B$ , and  $R$  of a pure light loss to the cell under the translational assumption we have been applying. As  $I_L$  lessens,  $V_{oc}$  undergoes a slight lessening also, due to the curve shift along the current axis and the negative slope at  $V_{oc}$ . The resultant parameters are plotted in Figures 3-14 and 3-15 versus  $I_L/I_{Lo}$ . The implications of a 10% coverslide darkening would be an apparent, but nonreal, increase to  $R/R_o$  of a factor of 2.2, a decrease in  $B/B_o$  of 0.987, and a decrease in  $A/A_o$  of 0.998. When corrections for various degrees of slide assembly losses are applied to the satellite parameters, a more recognizable cell degradation signature may be produced. Thus, cell and noncell losses might be distinguished by further detailed and careful study of parameter behavior.

The Second Quarterly Report previously discussed the separation of cell and non-cell losses with the hypothesis that noncell losses occurred primarily during the first few months on-orbit. Work is planned in the coming quarter to pursue both these approaches, for example, it should be interesting to examine the parametric signatures of degradation curves with the first 100 days omitted.

3-24

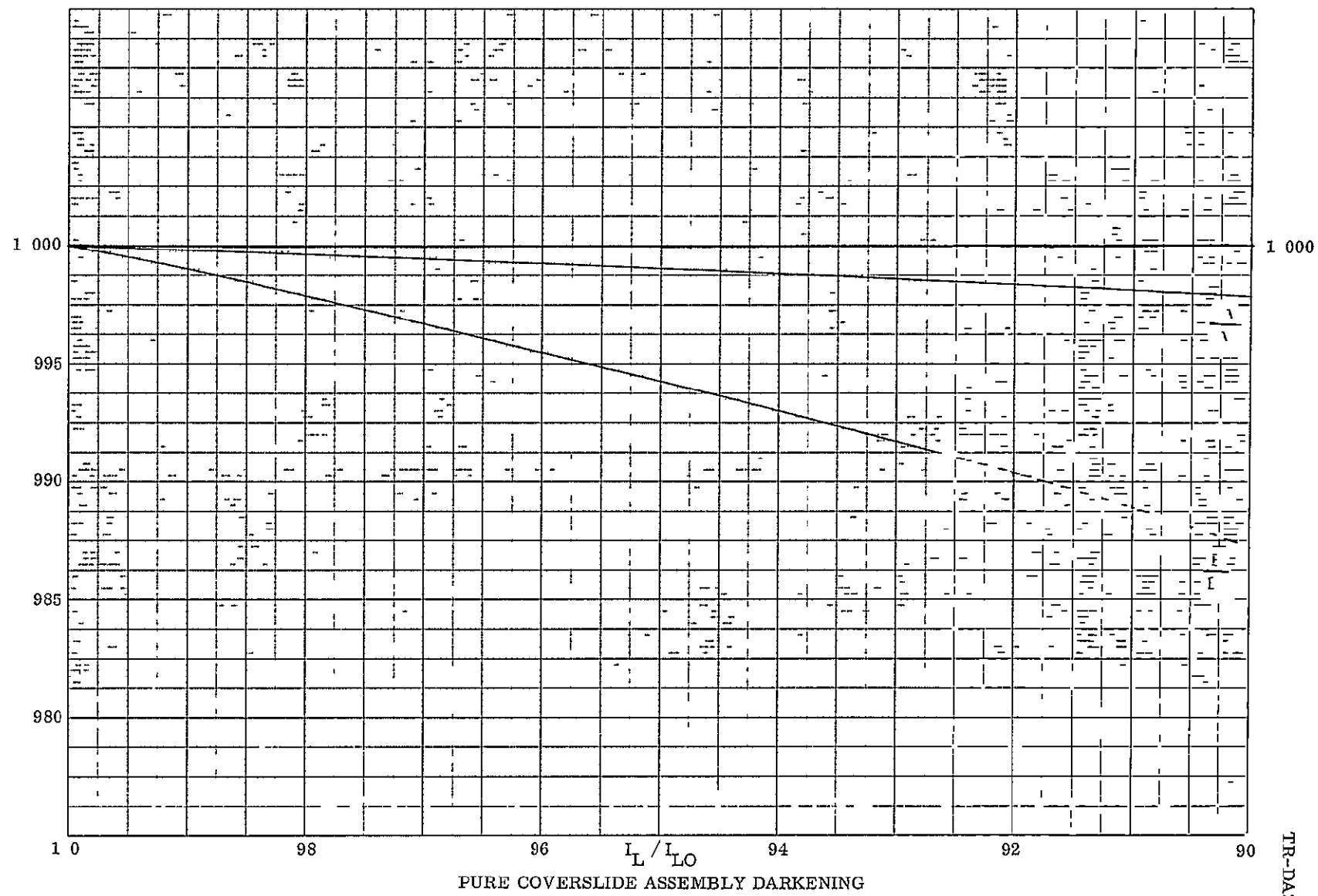
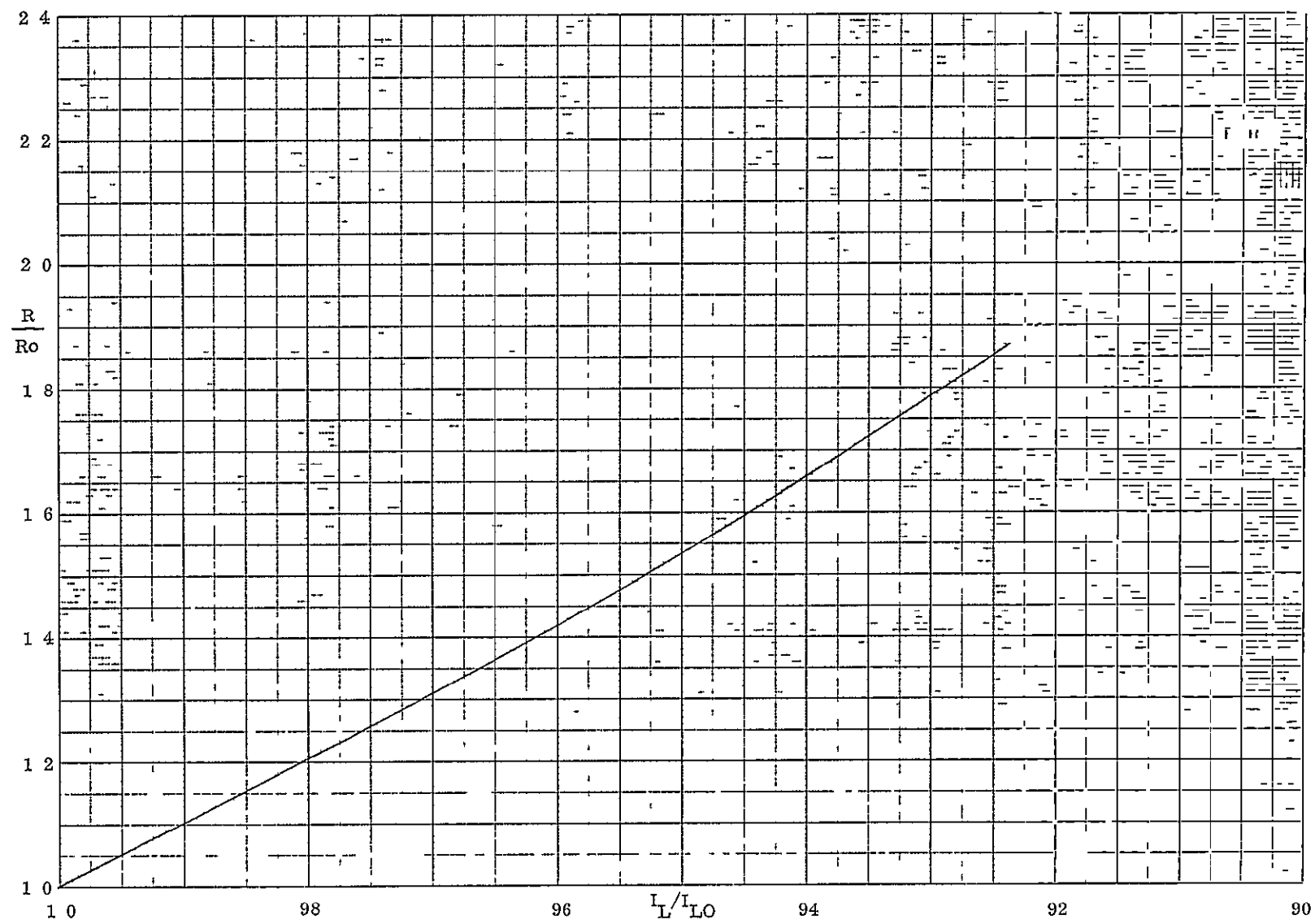


Figure 3-14 Effect on Parameters A and B of Pure Non-Cell Loss

3-25



PURE COVERSIDE ASSEMBLY DARKENING  
Figure 3-15 Effect on Parameter  $R$  of Pure Non-Cell Loss

TR-DA2179

SECTION 4 0

DETAILED RESULTS

## 4 1 UPDATE OF OBSERVED SOLAR FLARE PROTON SPECTRUM

The 1968 update of the solar proton observations at synchronous altitude<sup>(1)</sup> has been incorporated into our five-year average environment. The following table summarizes the available data.

Energy, E	Omnidirectional Fluence Greater than E (C <sub>m</sub> <sup>-2</sup> )		
	1967	1968	2-Yr Total
5 meV	1 37 x 10 <sup>9</sup>	3 71 x 10 <sup>9</sup>	5 08 x 10 <sup>9</sup>
21 meV	3 44 x 10 <sup>8</sup>	3 94 x 10 <sup>8</sup>	7 38 x 10 <sup>8</sup>

Figure 4-1 presents the 2-year integral spectrum above and the residual spectrum under the 20-mil coverslide shield. The extreme extrapolations shown in the figure were made for the purpose of solar cell degradation calculations but, as the following section will show, fluences at energies above 20 meV are negligible contributors to cell damage. The 5-year average flare environment was assumed to be 5/2 as great as the 2-year total shown above.

---

(1) G A Paulikas and J B Blake, Solar Observations at Synchronous during 1968, Aerospace Corporation Report No TR 0066 (5260 20) 13, December 1969

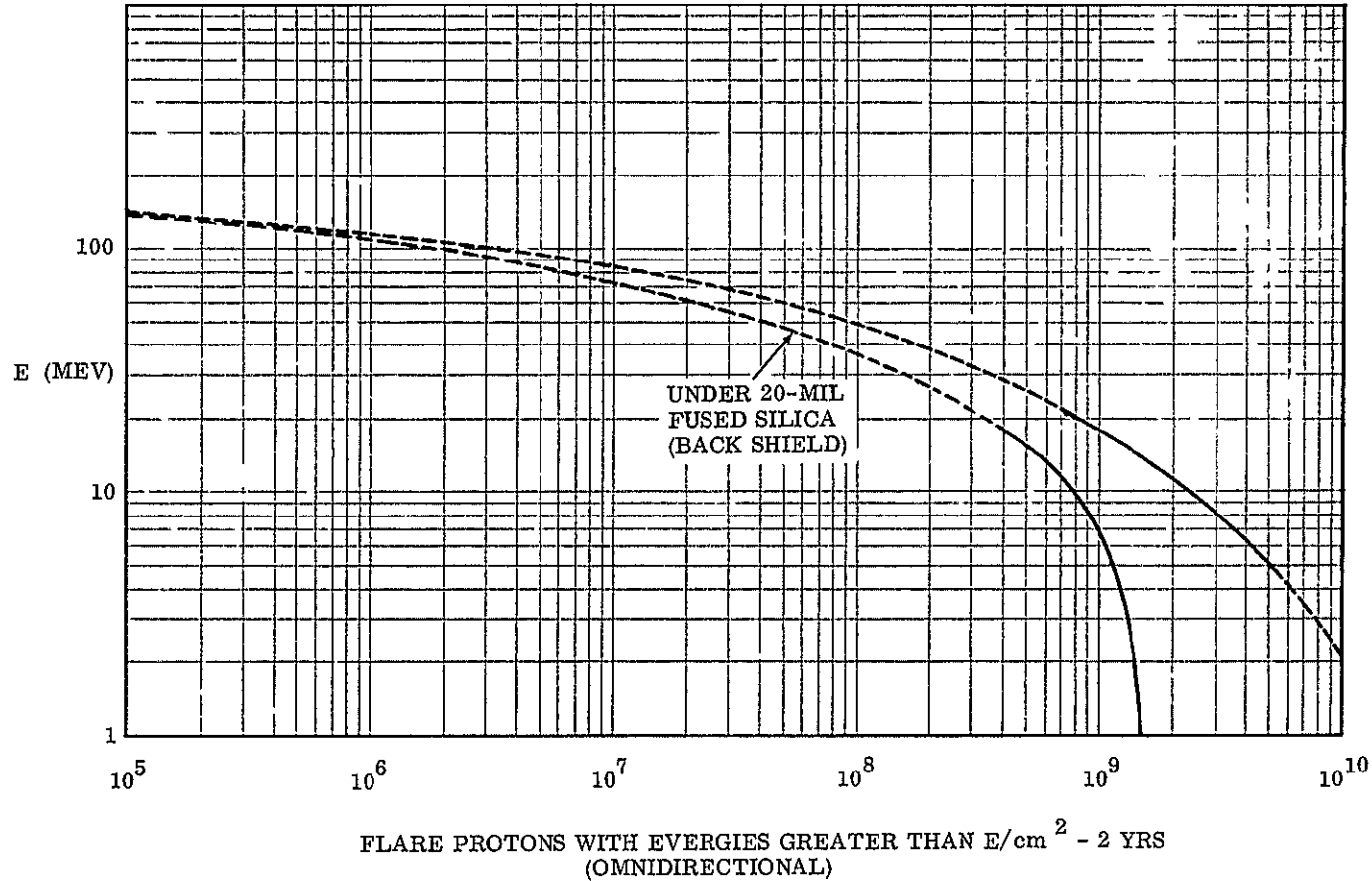


Figure 4-1 Average Flare Proton Environment for 1967 and 1968

## 4 2 CALCULATED RADIATION DEGRADATION

Incident particulate radiation, which sufficiently penetrates the solar cell, causes displacement damage in the crystal lattice which may be correlated to  $V_{oc}$  and  $I_{sc}$  degradation. Radiation is assumed to change the base region minority carrier lifetime which reduces the diffusion length  $L$  according to the relation,

$$\frac{1}{L^2} = \frac{1}{L_0^2} + K\phi$$

$K$  is an empirical damage constant which is dependent on energy and the type of radiation. When the incident radiation is a spectrum of energies, rather than monoenergetic, the simple product  $K\phi$  is best replaced by an integral or summation over the energy range. Values of the damage constants, and the correlations of  $L$  to  $V_{oc}$  and  $I_{sc}$  are taken from Cooley and Barrett<sup>(1)</sup>.  $L_0$  is assumed to be 200 microns.

Figure 4-2 and 4-3 show residual electron and proton spectra under the 20-mil coverslide in differential form. The plots present the number of particles/cm<sup>2</sup> in the energy region  $dE$  at  $E$ , as obtained from the previously published electron integral spectrum and the updated proton spectrum in Section 4-1. Figures 4-4 and 4-5 show the product  $K\phi$  as a function of energy, the maximum damage regions appear at energies near 0.7 meV for electrons and near 3 meV for protons. The areas under these curves represent the damage integral and have been evaluated by graphical summations. Five-year values appear below.

Radiation	$\int K\phi dE$	$L$ (5 yrs)	$I_{sc}/I_{sc}(0)$	$V_{oc}/V_{oc}(0)$
Electron	5600	111.1	0.954	0.972
Proton	2000	149.1	0.973	0.986
Combined	7600	99.5	0.940	0.965

Electron damage still dominates by a factor of roughly 5 to 2.

(1) W C Cooley and M J Barrett, Handbook of Space Environmental Effects on Solar Cell Power Systems, NASA Contract NASW 1345, 1968

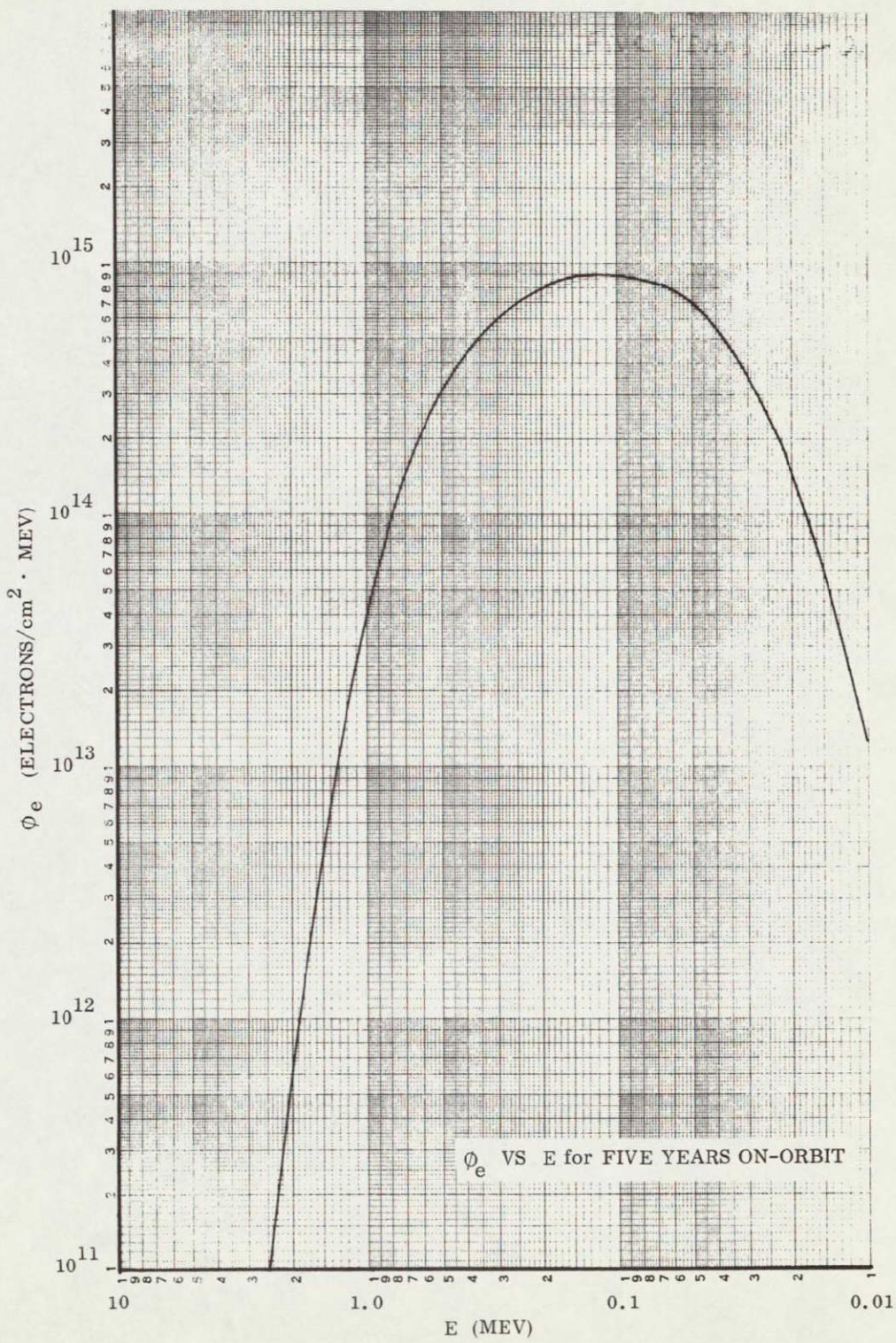


Figure 4-2 Residual Electron Differential Spectrum

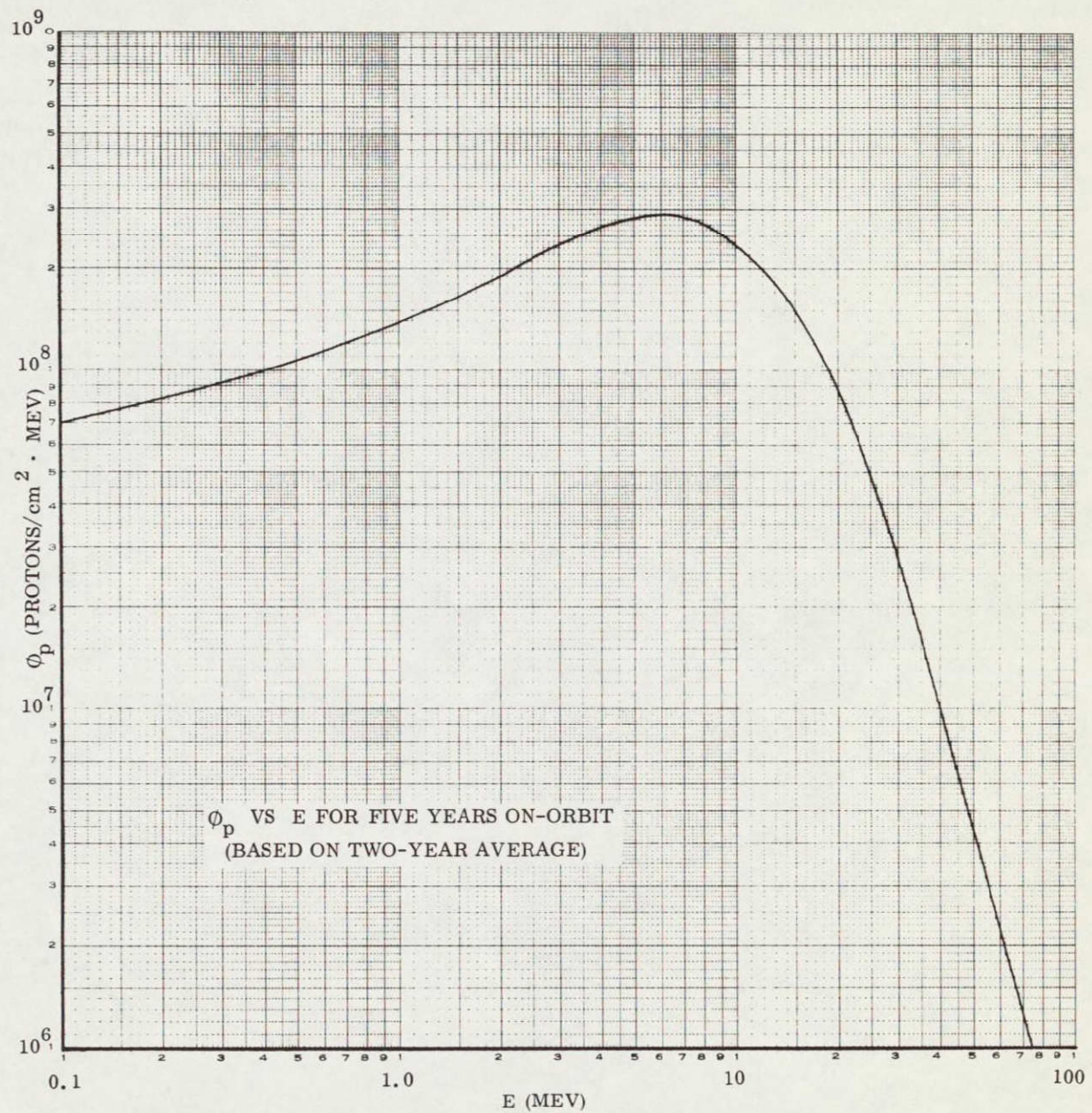


Figure 4-3 Residual Proton Differential Spectrum

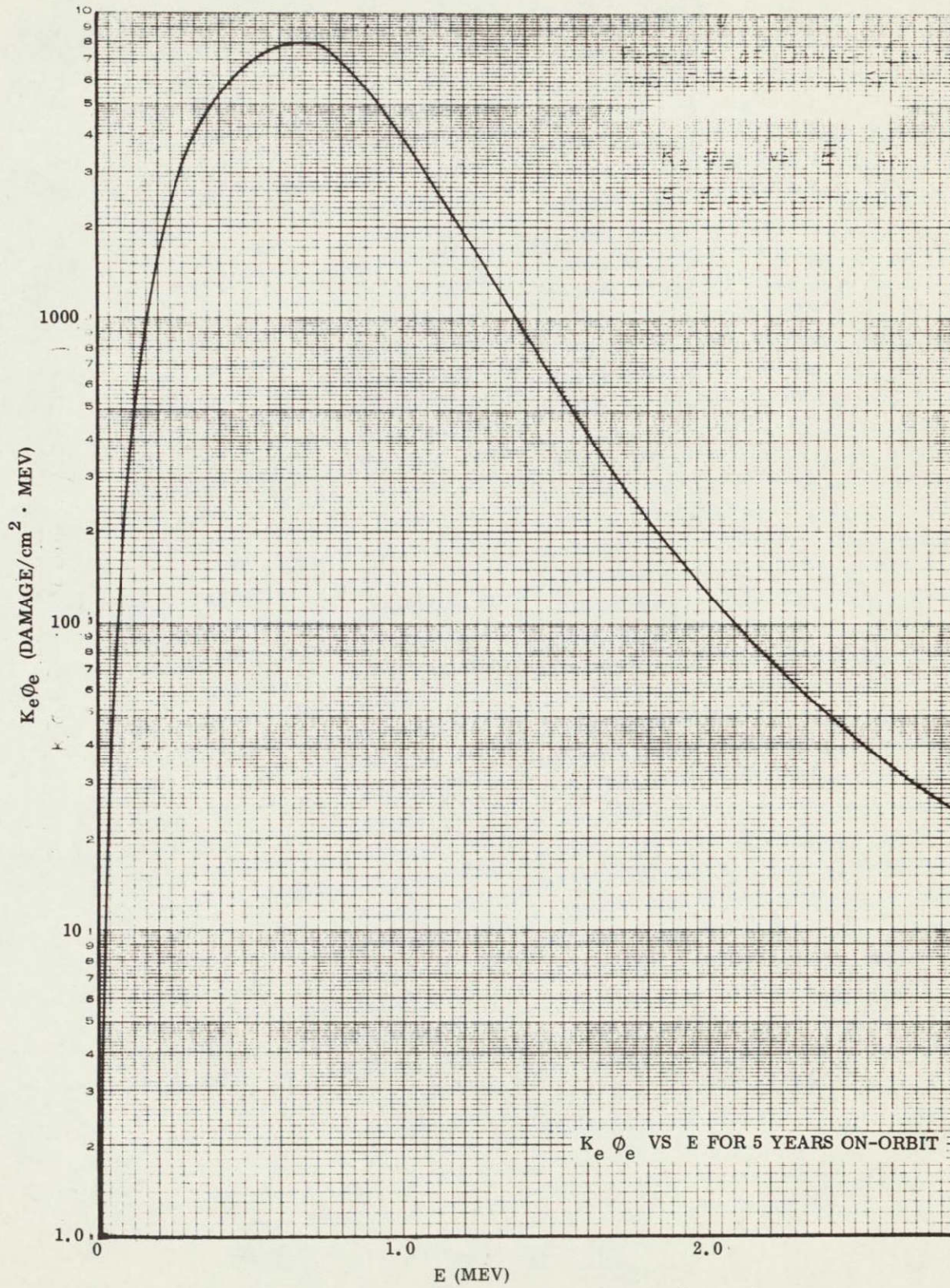


Figure 4-4 Product of Damage Constant and Differential Spectrum for Electrons

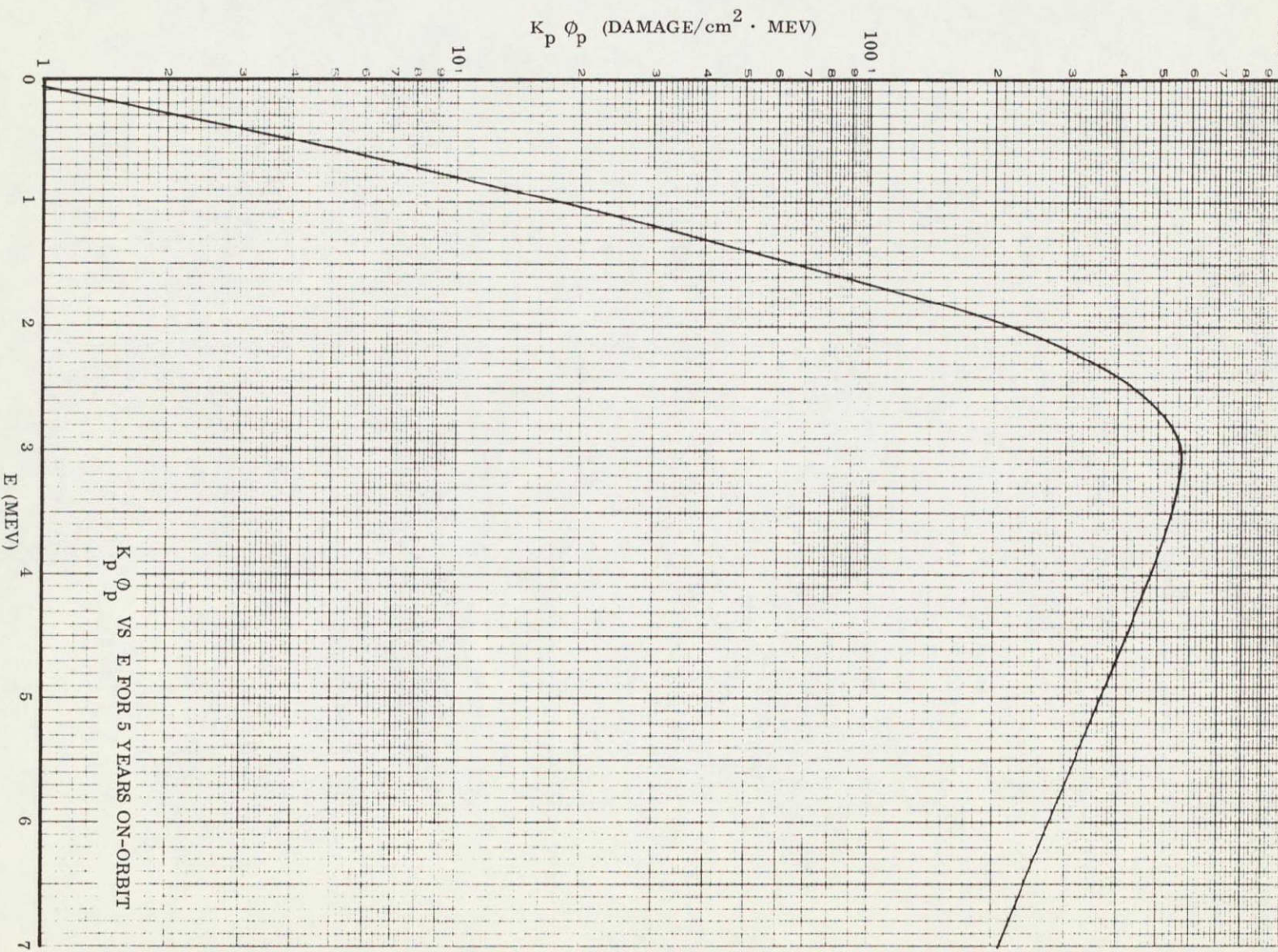


Figure 4-5 Product of Damage Constant and Differential Spectrum for Protons

## 4 3 PROJECTED OBSERVED DEGRADATION TO FIVE YEARS

The 15 IDSCS satellites launched on June 16, 1966, and January 18, 1967, have been analyzed to date with telemetry information spanning 3 29 and 2 68 years, respectively. The study has produced  $I_{sc}$  and  $V_{oc}$  ratios (e.g.,  $I_{sc}(t)/I_{sc}(0)$ ) of the output of an average individual solar cell assumed to be used throughout each array. A degradation function derived from theory, containing four parameters and time as an independent variable, was fit to each collection of ratios. A nonlinear regression program determined the optimum set of parameters to minimize the sum of the squares of the deviations of the points to the function. The complete table of regression parameters was published last quarter and is reprinted in Table 4-1. This table is currently being updated.

The functions and the regression parameters enable an extrapolation to be made which is dependent on every data point in the collection. A consequence of this is that updating will not only affect the curve at its endpoint, but will slightly revise the curve in its entirety. Third-launch satellites (three are transmitting telemetry) currently appear to be degrading at an accelerated rate, 5-year projections of  $I_{sc}$  appear to be 0.77, 0.79, and 0.79. These low values are more likely the result of our functional extrapolation technique than of actual behavior. The pros and cons of this technique are that every data point is used in the extrapolation but that small amounts of initial data cannot accurately establish curve shapes.

The functions used to represent the data have been discussed in the previous report and are

$$I_{sc}(t)/I_{sc}(0) = R_0 [1 - A \ln(1 + Bt)] (1 - Mt)$$

$$V_{oc}(t)/V_{oc}(0) = C \exp Kt$$

Table 4-2 normalizes all functions to unity at time zero and presents tabular past and projected degradation ratios. The notations X and N in the notation

TABLE 4-1  
REGRESSION PARAMETERS FOR PRESENT REGRESSION CURVES

Sat No	No of Points	R <sub>0</sub>	A	B	M	Corr Coeff	Square Error	C	K	Corr Coeff
9311		0 97894	0 0170906	0 0301294	4 6E-5	0 8961		0 98523	-1 09E-5	-0 23024
*9312	120	0 977313	0 034813	0 0130859	5 7664E-6	0 91480312	7 46E-3	0 98653502	-2 1143E-5	-0 7948
(-1st 100 days)		0 95465	0 059844	2 63098E-3			7 868042E-3			
9313	120	0 956	0 0245	8 6E-2	2 0E-5	0 8854	2 37E-2	0 9935	-2 36E-5	-0 410
(-1st 100 days)		0 900442	0 0970194	1 13878E-3			1 269E-2			
9314	61	0 96	0 0277	5 4E-2	1 8E-5	0 9267	8 8E-3	0 991	-9 2E-6	-0 1302
(-1st 152 days)		0 912696	0 0655155	0 00218011			0 002988974			
9315	119	0 9337	0 05389	5 05E-3	5 29E-6	0 8761	2 9E-2	0 991	-1 34E-5	-0 184
9316	120	0 9354	0 112	1 41E-3	7 334E-10	0 8819	4 18E-2	0 987	-1 198E-5	-0 156
9317	120	0 9501	0 1221	9 04E-4	1 771E-8	0 8374	3 16E-2	0 981	-1 73E-5	-0 276
9321	100	0 9845	0 0645	3 76E-3	2 51E-6	0 9451	9 67E-3	0 981	-1 2702E-5	-0 236
(-1st 100 days)		0 967373	0 108157	0 00129089			2 3671822E-3			
9322	100	0 944	0 0288	3 39E-2	8 71E-6	0 8308	2 66E-2	0 985	-1 96E-5	-0 509
*9323	99	1 00026	0 061752	4 64486E-3	0 0	0 94868836	4 16E-3	0 9896	-3 15E-5	-0 7888
*9324	99	0 982417	3 01126E-2	1 22619E-2	3 24663E-5	0 965984148		0 9877	-1 34E-5	-0 3072
*9325	97	0 959099	4 86362E-2	1 2289E-2	0 0	0 97150334		0 9957	-2 8E-5	-0 723
*9326	97	0 911331	5 2745E-2	7 50123E-3	0 0	0 9501903		0 9888	-3 1E-5	-0 731
*9327	100	0 971330E-1	4 48526E-2	1 11578E-2	0 0	0 96463641		0 993	-1 35E-5	-0 3322
*9328	100	0 898968	4 0419E-2	6 86838E-3	0 0	0 83381766		0 984	-3 21E-5	-0 4184
9331	8	0 989	8 63E-2	1 24E-2	1 0E-10		1 25E-3	0 998	-1 33E-4	-0 745
9332	81	0 97746	1 2E-2	4 145E-1	8 91E-5	0 9405	9 9E-3	0 987	-3 4E-5	-0 492
9333	82	0 96244	3 0E-2	1 7E-2	6 5E-5	0 9372	1 27E-2	0 98	-2 02E-5	-0 288
9334	82	0 995	9 3E-3	1 68E-1	9 17E-5	0 8901	1 77E-2	0 986	-3 23E-5	-0 468

\*Satellites have been run through revised non-linear regression for I<sub>sc</sub> data

Satellite No	$I_{sc}(t)/I_{sc}(0)$ for $t =$ (years)									$V_{oc}(t)/V_{oc}(0)$ for $t =$ (years)	Notation	
	0	0.1	0.2	0.5	1.0	2.0	3.0	5.0	1.0			
4-10	9311	1.0000	9857	9768	9599	9414	9146	8924	8530	9960	9803	
	9312	1.0000	9862	9762	9565	9369	9141	8992	8787	9923	9621	
	9313	1.0000	9645	9500	.9276	9081	8851	8689	8440	9914	9578	13 NVNI
	9314	1.0000	.9692	9545	9309	9100	8857	8690	8439	.9966	9833	14 XV
	9315	1.0000	9907	9827	.9639	.9418	9132	.8936	.8663	9951	9758	
	9316	1.0000	9944	.9890	.9743	.9535	9207	8954	8573	.9956	9784	
	9317	1.0000	.9960	9922	.9813	.9651	9381	9159	8810	.9937	.9689	17 XI
	9321	1.0000	9916	.9842	9658	9434	9131	.8922	.8630	9954	9771	21 XV
	9322	1.0000	.9765	.9635	9417	9224	9007	8866	8667	.9929	.9648	
	9323	1.0000	.9903	9820	9621	9387	9086	.8884	.8611	9886	.9441	
	9324	1.0000	9877	9784	9589	9375	.9087	8869	8514	9951	9758	
	9325	1.0000	9820	9688	9428	.9172	8881	8701	8466	9898	.9502	25 NI
	9326	1.0000	9872	9770	9545	.9304	.9014	8828	8582	9887	9450	
	9327	1.0000	9847	9733	9502	9271	9007	.8842	8626	9951	9756	
	9328	1.0000	9910	.9836	.9671	.9493	9275	9134	.8947	.9883	9431	28 XINV

column refer to maximum and minimum 5-year values as used elsewhere in the report, 25 NI indicates that it is Satellite No 9325 that has the minimum short-circuit current value of all second launch satellites. Further values of the open-circuit voltage ratio may be obtained by evaluating the simple exponential function with the parameter K taken from Table 4-1. In a semi-log plotting (with time on the linear axis), two points are sufficient to establish the curve

## 4 4 TELEMETRY ERROR ANALYSIS

4 4 1 Sources of Error

There are two types of error, systematic or fixed error and random error. The latter is of primary concern for this work. All degradation ratios are normalized to start-of-life, so systematic errors will influence only absolute quantities, while the random errors can affect the degradation ratio points.

Our task is further simplified by the results of using a reference analog voltage as a means of testing the stability of the telemetry system. Data show the reference signal to be constant to within  $\pm 0.78\%$  for the resolution of the system, thus, we can assume the errors introduced by the telemetry system are negligible. Therefore, we must concern ourselves with the stability of the sensors of each data channel providing information used in the degradation analysis.

4.4.2 Worst-Case Approach

All sensors operate within worst-case stability specifications as listed below.

- a. Voltage Sensors                     $\pm 2\%$  of full scale in 3 years
- b. Current Sensors                     $\pm 2\%$  of full scale in 3 years
- c. Temperature Sensors               $\pm 3^\circ\text{C}$  in 3 years (negligible)
- d. Aspect Sensors                     $< 0.1^\circ$  in 3 years (negligible)

The RMS quantization error for a binary system is given by

$$Q. E. = \pm \frac{1}{2^{n+1}\sqrt{3}}, \quad \text{where } n = \text{number of bits/word}$$

$$Q. E. = - \frac{1}{2^7\sqrt{3}} = \pm 0.45\%$$

The total RMS error is then for each parameter

a      Voltage       $T_V = \sqrt{2^2 + (45)^2 + (78)^2} = \pm 2.19\%$

b      Current       $T_I = \sqrt{2^2 + (45)^2 + (78)^2} = \pm 2.19\%$

The electrical parameters of concern and associated instabilities in engineering units are as follows

a      Control Bus Voltage	(14.7 vfs)      ( $\pm 2.19\%$ )	= $\pm 322$ mV	
b      Control Bus Current	(1000 ma)	( $\pm 2.19\%$ )	= $\pm 22$ ma
c      Main Bus Current	(2000 ma)	( $\pm 2.19\%$ )	= $\pm 43.8$ ma

#### 4.4.3 Influence of Worst-Case Instabilities on Degradation Data

To establish stability bounds on the results of the  $I_{SC}$  and  $V_{OC}$  degradation analysis, the worst-case stability margins for the sensors in Paragraph 4.4.2 were introduced in the analysis. The combined instabilities produce a translation of about  $\pm 4\%$  in the function fitted to the  $I_{SC}$  degradation data. The  $V_{OC}$  degradation is translated by about  $\pm 0.1\%$ .

#### 4.4.4 Observed Sensor Stabilities

During illuminated periods, the array sees essentially a constant power load. Telemetry data indicate no shift in either main bus current or voltage within the resolution limits of the system. This indicates sensor stability within the resolution of the system, or

a $T_V$	= $\pm 0.19\%$
b $T_I$	= $\pm 0.19\%$
c. $T_{Temp}$	= $\pm 0.19\%$

This instability is considered negligible in its effect on degradation data.

#### 4.4.5 Conclusions

The influence of telemetry and sensor instabilities on degradation information is negligible

#### 4.5 COMPARISON OF OTHER FLIGHT DATA

Since 1963 there have been approximately 45 satellites launched into geostationary orbits. Twenty-seven of these are IDSCS satellites, 19 of which are the subjects of this study. Barring a few exceptions, there is a sparsity of published information on the performance of the solar arrays utilized on the remaining synchronous spacecraft. An analysis of an array's performance demands sufficient information to develop a complete I-V curve, this requires data near the short-circuit current, open-circuit voltage, and knee of the I-V curve. Few satellites have had the necessary instrumentation to provide these data. One might question the economics of this type of thinking when these potential sources are available and accurate degradation data are still urgently needed for future array designs. Though the present comparison of available flight data is still in progress, preliminary work to date is presented here.

Figures 4-6 through 4-8 represent the short-circuit current degradation, open-circuit voltage degradation, and maximum power point degradation of the satellites considered. These include the best- and worst-case examples of the first two IDSCS launches, Intelsat I, Intelsat II, F-3, and Cell #23 in the ATS-1 solar cell experiment. The ATS-1 experiment included various shield thicknesses. Cell #23 in the experiment had a 15-mil shield which most closely approximates the 20-mil shields used on IDSCS arrays. The degradation after 416.8 days (1.142 years), as presented by Waddel<sup>(1)</sup>, is indicated by the single point shown in Figures 4-6, 4-7, and 4-8. As only two points are presented, no attempt is made to extrapolate resulting curves and no trend can be shown. After slightly more than one year, this cell degrades in  $I_{sc}$ ,  $V_{oc}$ , and  $P_{max}$  to correspond closely with the best- and worst-case degradation seen in IDSCS.

Intelsat I, as reported by Curtin<sup>(2)</sup>, shows a markedly greater loss in  $P_{max}$  initially than is found in the other satellites. At the 4-year point, however, it is within 1% of IDSCS 9313 and 9325.

- (1) "Solar Cell Radiation Damage on Synchronous Satellite ATS-1," R. C. Waddel NASA/Goddard Space Flight Center, X-710 68-408, October 1968
- (2) "Evaluation of the performance of Solar Arrays in Intelsat Spacecraft at Synchronous Altitude," D. J. Curtin, J. F. Stockel, Comsat Corp., Wash., D. C., 4th IECEC, Sept. 22-26, 1969, A69-42287

Intelsat II, F-3, shows a  $V_{oc}$  loss several percent greater than found in IDSCS, while its  $I_{sc}$  loss corresponds well with the worst-case IDSCS satellites

Work is presently underway to examine parametrically the degradation of these and other satellites. It is hoped that such an analysis will further clarify the mechanisms responsible for the variation in degradation rates, thus, trends found on the IDSCS arrays may be compared on a more physical basis with other flights

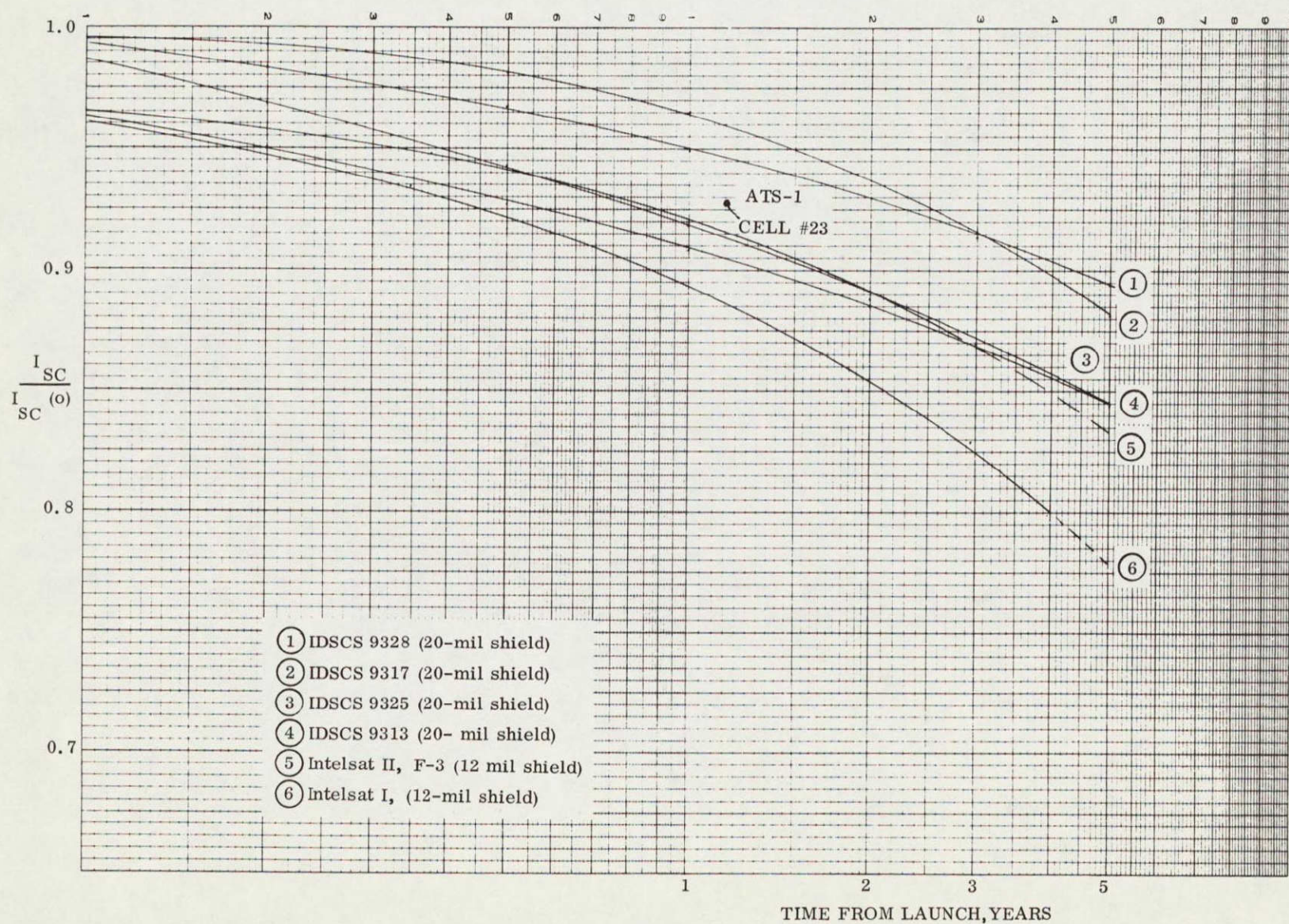
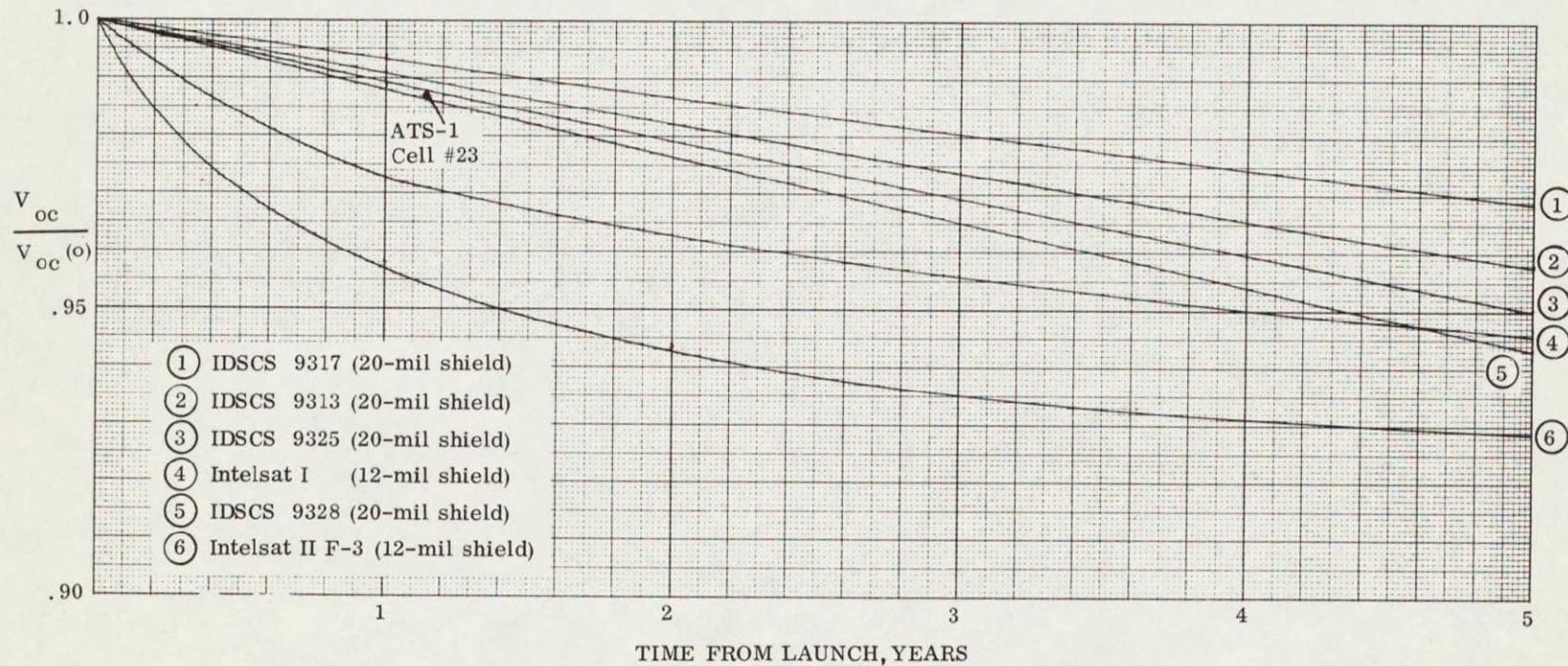
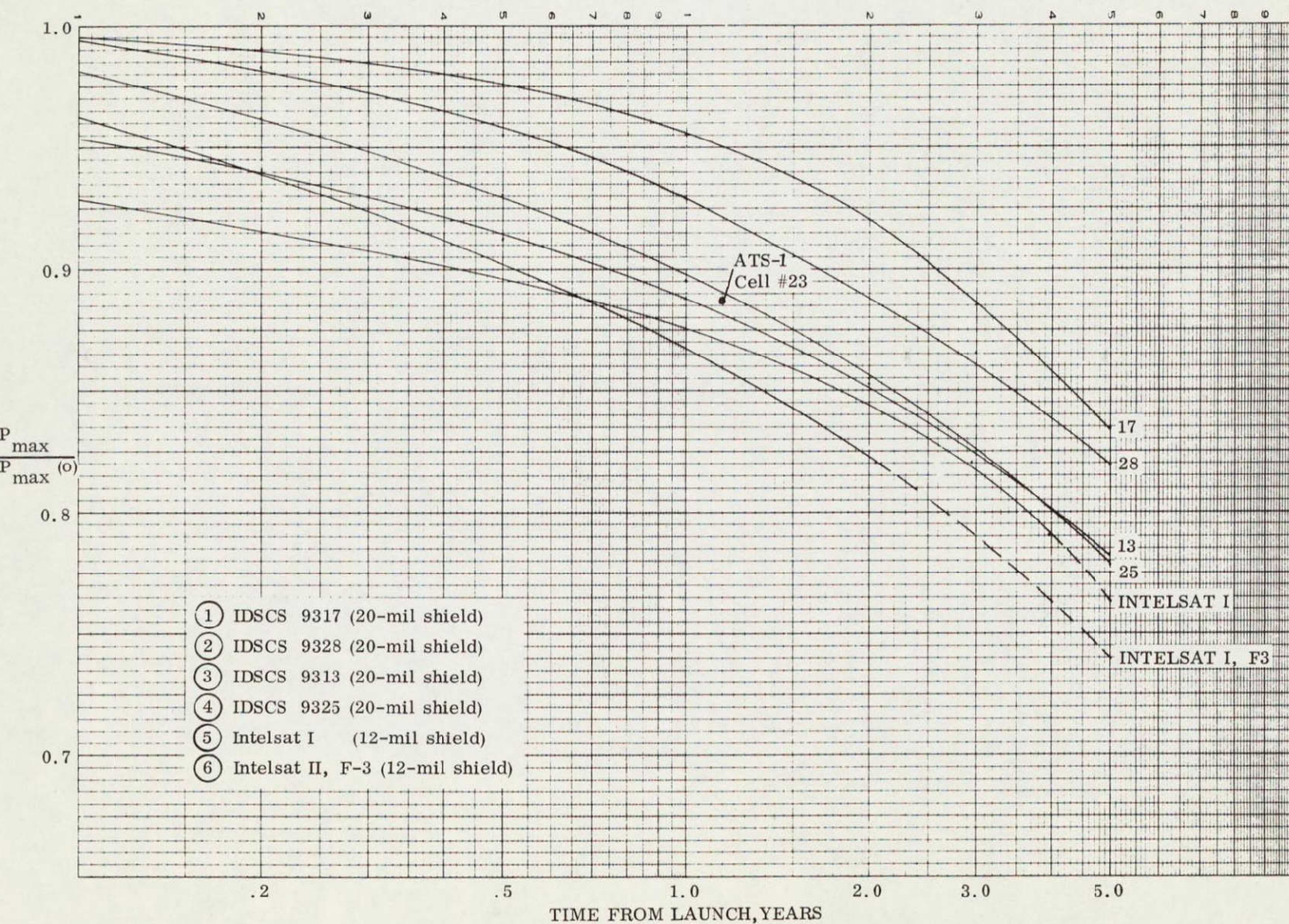


Figure 4-6 Comparison of  $I_{SC}$  Degradation

Figure 4-7 Comparison of  $V_{oc}$  Degradation

END

4-19



**PHILCO** 

**SPACE & RE-ENTRY SYSTEMS DIVISION**  
**Philco-Ford Corporation**  
**Palo Alto, California 94303**

